HHS Public Access

Author manuscript

Nat Commun. Author manuscript; available in PMC 2015 May 27.

Published in final edited form as:

Nat Commun. ; 5: 5567. doi:10.1038/ncomms6567.

A Genetic Variant of p53 Restricts the Mucus Secretory Phenotype by Regulating SPDEF and Bcl-2 Expression

Hitendra S. Chand[1], **Gilbert Montano**[1], **Xuesong Huang**[1], **Scott H. Randell**[2], **Yohannes Mebratu**[1], **Hans Petersen**[1], and **Yohannes Tesfaigzi**[1]

[1]COPD Program, Lovelace Respiratory Research Institute, Albuquerque, NM 87108, USA

[2]Department of Cell and Molecular Physiology, The University of North Carolina, Chapel Hill, NC 27599, USA

Abstract

Despite implications for carcinogenesis and other chronic diseases, basic mechanisms of p53 and its variants in suppressing Bcl-2 levels, are poorly understood. Bcl-2 sustains mucous cell metaplasia, whereas *p53*$^{-/-}$ mice display chronically increased mucous cells. Here we show that p53 decreases *bcl-2* mRNA half-life by interacting with the 5' untranslated region (UTR). The p53-*bcl-2* mRNA interaction is modified by the substitution of proline by arginine within the p53 proline-rich domain (PRD). Accordingly, more mucous cells are present in primary human airway cultures with p53^{Arg} compared with p53^{Pro}. Also, the p53^{Arg} compared with p53^{Pro} displays higher affinity to and activates the promoter region of SAM-pointed domain-containing Ets-like factor (SPDEF), a driver of mucous differentiation. On two genetic backgrounds, mice with targeted replacement of prolines in p53 PRD show enhanced expression of SPDEF and Bcl-2 and mucous cell metaplasia. Together, these studies define the PRD of p53 as a determinant for chronic mucus hypersecretion.

Introduction

The importance of Bcl-2 and its family members in cell survival, differentiation, and oncogenesis has been demonstrated extensively. Bcl-2 overexpression inhibits cell death and can promote cell transformation when present together with mutations of certain oncogenes[1,2]. For example, combined expression of Bcl-2 and c-Myc leads to the rapid transformation of lymphocytes and other cell types[3,4]. Consistent with its oncogenic function, Bcl-2 is aberrantly overexpressed in a wide range of human tumors, including B-

Corresponding Author: Yohannes Tesfaigzi, Lovelace Respiratory Research Institute, 2425 Ridgecrest Dr. SE, Albuquerque, NM 87108, Tel: (505) 348-9495, Fax: (505) 348-8567, ytesfaig@LRRI.org.

Authors Contributions

HSC and YT designed the experiments. HSC, GM, and XH performed and analyzed the experiments. SHR and HP assisted and analyzed the experiments. YT conceived and designed the study. The manuscript was written by HSC and YT with assistance from other authors.

Competing Financial Interest Statement

The authors declare no competing financial interests.

cell and T-cell lymphomas[5] and non small cell lung carcinomas[6]. This central gate-keeping role of Bcl-2 necessitates a highly controlled regulation of its expression. Despite its functional importance, the molecular mechanisms regulating Bcl-2 expression are largely unknown.

We and others have reported on evidence that p53 affects transcriptional activity of a partial Bcl-2 promoter in pulmonary epithelial cells[7–9], which was consistent with numerous studies reporting that p53 acts as a transcription factor[10]. The *bcl-2* gene is composed of 3 exons whereby exons 1 and 2 are separated by a long intron of 150kb[11]. Exon 1 contains the 5' up-stream region with promoters P1 and P2 and part of the protein coding open reading frame (ORF)[12]. Exon-2 encodes for parts of the ORF and the 3'UTR and the remainder of which is encoded by exon 3. The P2 promoter region contains a CCAAT box and a TATA element and is the primary suppressor of the P1 promoter. This negative regulatory region is highly conserved across species and may be modulated by the M region of the *bcl-2* promoter[13].

Our previous studies show that pulmonary inflammation initiates airway epithelial cell proliferation and Bcl-2 expression in proliferating epithelial cells[14,15]. Gain- and loss-of-function studies showed that Bcl-2 expression sustains hyperplastic epithelial cells, and Bcl-2 expression is elevated in airway mucous cells of subjects with cystic fibrosis[16], in patients with chronic mucous hypersecretion (CMH)[17], and in airway epithelium of asthmatics[18].

Chronic obstructive pulmonary disease (COPD) encompasses a spectrum of diseases, with chronic bronchitis (CB) at one end and emphysema at the other. The classic definition for CB is chronic cough and sputum production for at least 3 months per year for two consecutive years[19]; although it is not clear whether CB is a disease of large airways only or whether inflammation in small airways causes mucous cell metaplasia that plays a distinct role in the development of CB. While all smokers develop an inflammatory response, CB is only observed in a subset of heavy smokers[20], and in approximately half of these individuals CB persists even after quitting smoking[21]. Smokers with CB are at higher risk of increased exacerbation rate[22], longer recovery period following acute COPD exacerbations[23], worse health-related quality of life including general health status, severe respiratory symptoms, increased physical activity limitation[24], and have worse lung function[25]. In addition, among subjects with COPD, those with CB are at higher risk for accelerated decline in lung function[34], and lung cancer[26,27], and are prone to increased mortality[23], especially after lung volume reduction surgery[28]. Persistent CB in former smokers may be due to some intrinsic factors such as susceptibility genes that predispose them to this condition. Therefore, intervention strategies for reducing CB requires identification of endogenous factors including genetic polymorphisms that make smokers susceptible to sustained chronic mucous hypersecretion.

In the present study, we show that when Bcl-2 regulation is analyzed in the context of the entire promoter construct, p53 primarily regulates Bcl-2 levels by reducing the mRNA half-life rather than affecting promoter activity. When studying the detailed mechanisms of p53-induced suppression of Bcl-2 regulation and how that may affect the role of sustaining

metaplastic mucous cells, we determined that two p53 variants, due to a polymorphism at codon 72, differentially affect *bcl-2* mRNA half-life and are associated with increased CB in smokers. In addition, microarray expression analysis of primary human airway epithelial cells (HAECs) homozygote for the two genotypes pointed to the differential regulation of SPDEF, a protein that is sufficient and necessary to drive the mucous regulatory phenotype in airway cells. Both the high mucous secretory phenotype and increased Bcl-2 and SPDEF levels were also observed in mice when the highly conserved proline-rich domain of p53, where the corresponding human variant resides, was modified. Together, these studies provide the fundamental understanding of chronic mucous hypersecretion and may help not only the detection and early management of this debilitating disease but also the development of effective therapies.

Results

Absence of p53 prolongs mucous cell metaplasia

Our previous studies have shown that Bcl-2 is expressed in metaplastic mucous cells in various animal models of chronic bronchitis and asthma[14,15,29]. Furthermore, we have shown that Bcl-2 sustains metaplastic mucous cells[16] and that p53 is involved in regulating Bcl-2 expression[13]. To investigate whether the regulation of Bcl-2 by p53 translates into modification of mucous cell metaplasia, the extent of MCM in airway epithelia at airway generations 3, 4, and 5 was quantified in $p53^{+/+}$ and $p53^{-/-}$ mice at 5, 8, and 12 d after intranasal instillations of LPS. In $p53^{+/+}$ mice the numbers of mucous cells/mm basal lamina were increased at 5 and 8 d post instillation and returned to baseline at 12 d (Fig. 1A). However, in $p53^{-/-}$ mice MCM remained elevated at 12 d and was higher than that observed in $p53^{+/+}$ at the same time point (Fig. 1A). Immunostaining of lung tissue sections from $p53^{+/+}$ and $p53^{-/-}$ mice at 12 d post LPS instillation showed that Bcl-2 and Muc5ac positivity was significantly higher in $p53^{-/-}$ mice (Fig. 1B) both when quantified as percentage of total epithelial cells or as numbers/mm basal lamina (Fig. 1C, D). These results suggest that Bcl-2 expression was sustained in $p53^{-/-}$ mice causing persistent MCM, while Bcl-2 was downregulated in $p53^{+/+}$ mice allowing the resolution of MCM at 12 d.

p53 affects *bcl-2* mRNA levels and stability

Several studies have documented a suppressive effect of p53 on Bcl-2[8,9] and an inverse correlation of p53 and Bcl-2 levels for squamous lung cancers[30]. Consistent with these reports, the p53-sufficient H23 and AALEB cells showed reduced *bcl-2* mRNA and protein levels compared to p53-deficient SAOS-2 cells (Supplementary Fig. 1A, B). These results were further confirmed in p53-deficient SAOS-2 cells stably expressing p53 or the respective controls (Supplementary Fig. 1C) and in H1299 cells that were stably transfected with a temperature-sensitive form of p53 (H1299p53^{ts}) (Supplementary Fig. 1D). Similarly, HCT116 cells deficient in p53 (Fig. 2A) and primary murine airway epithelial cells (MAECs) from $p53^{-/-}$ mice (Fig. 2D) expressed increased *bcl-2* mRNA levels compared to the respective wild-type controls.

We previously observed that the P2 promoter region of the *bcl-2* gene, when analyzed alone or in the absence of P1 or M regions, interacts with and was suppressed by p53[13]. To further

evaluate the effect of p53 on P2 promoter activity in the context of the full-length promoter that contains the P1, M, and P2 regions, we compared the promoter activities of constructs containing the progressively deleted P2 region in p53-sufficient A549 and p53-deficient H1299 cells (Supplementary Table 1). The activities of the P1-M-P2 promoter were lower in both cells lines when > 140 bp of the P2 region was present (Supplementary Fig. 2A). Similarly, when the same constructs were tested in H1299 cells stably transfected with the temperature-sensitive p53 ($p53^{ts}$), the P2 region effectively reduced promoter activity regardless of the p53 activation status (Supplementary Fig. 2B). The promoter activity assays repeatedly showed that p53 minimally suppressed *bcl-2* promoter activity, and removal of the entire P2 region affected promoter activity only by a factor of 2–3. In fact, promoter activity appeared to be increased when p53 was activated at 32°C (Supplementary Fig. 2B). These findings did not adequately explain the >10-fold suppression of Bcl-2 expression by p53.

To further evaluate the reason for reduced Bcl-2 levels in p53-sufficient cells, we investigated whether p53 may affect *bcl-2* mRNA stability. *Bcl-2* mRNA half-life was significantly longer in the p53-deficient H1299 and SAOS-2 cells compared to the p53-sufficent A549 and AALEB cells (Supplementary Fig 2C). The effect of p53 was further confirmed by the observation that *bcl-2* mRNA half-life was longer in $p53^{-/-}$ HCT116 cells and in primary MAECs from $p53^{-/-}$ mice compared to the $p53^{+/+}$ counterparts (Fig. 2B, E and Supplementary Fig. 2D, E). This shorter half-life in *bcl-2* mRNA translated into lower Bcl-2 protein levels in p53 sufficient HCT116 p53-deficient cells (Fig. 2C). Together, these results showed that p53 enhances the degradation of *bcl-2* mRNA.

p53 interacts with the P2 region within the 5'UTR of *bcl-2* mRNA

While the role of p53 as a transcriptional regulator is extensively studied, the role of p53 in regulating mRNA stability is unknown. Because p53 affected *bcl-2* mRNA stability and p53 interacted with the P2 region, we investigated whether this region is part of the 5'UTR of *bcl-2* mRNA. Because mechanisms involving immortalization can introduce possible artifacts in cell lines, we investigated whether the 5'UTR also extends to the P1 region by preparing *bcl-2* RNA from primary HAECs and mapping the transcriptional start sites using 5'RACE. Primers designed to amplify various regions within the 5'UTR identified four different transcriptional start sites: T1, T2, T3, and T4. Sequence analysis revealed that T1 and T2 originate within the P1 region at −1778 and −1313, respectively (Supplementary Fig. 3A). T3 and T4 were localized within the P2 region of *bcl-2* gene, and transcriptional start sites were mapped to nucleotides −465 and −176 upstream of the open reading frame, respectively (Supplementary Fig. 3A). To further validate the findings from the 5'RACE, we used primers specific to either P2 or M regions for RT-PCR using DNase-treated RNA that was isolated from various epithelial cell lines. Both sets of primers successfully amplified products specific to the P2 (Supplementary Fig. 3B) and M (Supplementary Fig. 3C) regions in RNA isolated from AALEB and SAOS-2 cell lines. These findings further confirmed that P2 sequences are part of the Bcl-2 transcript not only in primary cells, but also in other cell types assayed, including cancer cells.

We also investigated whether P2 sequences are transcribed when they are present as promoter-luciferase constructs in which sequences representing the 3'UTR are excluded. The P2 and M regions were detected by RT-PCR in A549 and H1299 cells that were transfected with luciferase constructs containing P1-M-P2 or P2 promoter regions using forward primers specific for P2 or M and luciferase cDNA-specific reverse primers (Supplementary Fig. 3D, E, F). Collectively, our findings confirmed that sequences of P2 region are represented within the 5'UTR of Bcl-2 transcripts in several cell lines and that the absence of 3'UTR sequences of *bcl-2* mRNA did not affect the transcriptional start site of *bcl-2* gene.

In addition, the *bcl-2* transcripts for T1, T2, T3, and T4 were successfully amplified by RT-PCR using specific primers designed within the 5'UTR (Fig. 2F). These results demonstrate that p53 interacts with the *bcl-2* transcripts and suggest that P2 sequences on *bcl-2* mRNA could represent sites of interaction with p53. Because our results demonstrated that P2 sequences are part of *bcl-2* mRNA 5'UTR, we next investigated whether p53 interacts with *bcl-2* mRNA.

A P2 region mediates p53-dependent destabilization of *bcl-2* mRNA

The interaction of p53 with the 5'UTR suggested that the P2 region is responsible for the p53-dependent degradation of *bcl-2* mRNA. Previous findings have reported that the critical region for p53 interaction with the Bcl-2 promoter lies within P2 region[8,13,31]. To identify 5'UTR sequences within *bcl-2* mRNA that are responsible for p53-dependent *bcl-2* mRNA decay, HCT116p53$^{+/+}$ cells were transfected with P1-M-P2 luciferase constructs that contain progressive deletions within P2 (Supplemental Information, Table 1). Luciferase mRNA half-life (Fig. 2G and Supplementary 2F) and luciferase activity (Fig. 2H) were reduced drastically from ~4.5 h in P1-M-P2Δ4 to ~1–2 h in P1-M-P2Δ5 construct, suggesting that the deleted 66 nucleotides (regions –423 to –489) in P1-M-P2Δ5 were important for p53-dependant RNA degradation.

To confirm that the 66-nucleotide region interacts with p53, we first conducted RNA pull down assays using *in vitro* transcribed *bcl-2* mRNA. For this purpose, we subcloned the P2 fragment into the PCR2.1 dual promoter vector to generate sense and anti-sense biotinylated mRNAs and found that p53 was only detected in pull-down products using sense mRNA (Supplementary Fig. 3G). Hence, interaction of p53 with *bcl-2* mRNA was confirmed by both p53 antibody and *bcl-2* mRNA pull-downs.

These results were confirmed by *in vitro* RNA pull-down assays using a short synthetic 50 nucleotide construct that comprises nucleotides −443/−429. To further delimit the site of interaction, mutations were introduced by changing the first or second 8 nucleotides or by modifying the 16 nucleotides in sets of 4 nucleotides (representing the 16 nucleotides in P2–443/−429) to random sequences as shown in Supplementary Table 2. All of the mutations disrupted p53 interaction with this region because *in vitro* RNA prepared from a control nucleotide sequence within the P2 region (−608/−582) did not show p53 binding suggesting that the interaction is specific to these 16 nucleotide sequence (Supplementary Fig. 3H). To further characterize the sequences within the 66 nucleotide region that interact with p53, two deletion mutants, P2Δ−482/−468 and P2Δ−443/−429 were generated using site-directed

mutagenesis. RNA pull-down assays using these deletion mutants revealed that the 16 nucleotides (−443/−429) were important for the interaction with p53 (Fig. 2I).

To determine the influence of these nucleotides on mRNA half-life *in vivo*, we deleted the corresponding sequence in P1-M-P2 to generate P1-M-P2Δ(−443/−429)-luciferase construct and compared the luciferase mRNA half-life following transfection of HCT116p53$^{+/+}$ cells. The luciferase mRNA half-life (Fig. 2J and Supplementary Fig. 2G) and luciferase activity were increased by approximately 2-fold (Fig. 2L) for the P1-M-P2 compared to the P1-M-P2Δ(−443/−429) luciferase constructs, respectively, suggesting that p53 must interact with these sequences to destabilize the mRNA. Furthermore, introducing 4 nucleotide mutations at loci −443/−439 and −433/−429 within the P1-M-P2-luciferase construct did not affect luciferase mRNA half-life (Fig. 2J and Supplementary Fig. 2G), suggesting that merely mutating 4 nucleotides is not sufficient to completely abrogate the interaction of p53 in cells. Overall, these results show that the 16 nucleotide region within P2 is crucial for the interaction of p53 with the *bcl-2* mRNA. This reduction in *bcl-2* mRNA half-life by p53^{Pro} suggests that the PRD of p53 plays an important role in this decay process. To further study the possible differences in the interaction of p53^{Arg} and p53^{Pro} with *bcl-2* mRNA, we performed a pull-down assay using p53 antibody or IgG_1 as control from H1299 parent cells, H1299p53^{ts}Arg, and H1299p53^{ts}Pro cells. p53 was absent in the parent H1299 cells and *bcl-2* mRNA was greater in pull-down products from H1299p53^{ts}Arg compared to H1299p53^{ts}Pro cells even when normalizing for the reduced p53^{Pro} levels detected in the pull-down products (Fig. 2L), supporting the idea that p53^{Arg} has a higher affinity to the *bcl-2* mRNA than p53^{Pro}.

Genetic variation in p53 is associated with mucous hypersecretion

Because Bcl-2 sustains mucous cells that may be responsible for increased mucous hypersecretion in chronic diseases, such as cystic fibrosis[16] and chronic bronchitis[29], we wanted to investigate whether the differential regulation of Bcl-2 by p53 could be associated with increased chronic mucous hypersecretion in humans. First, we tested whether we can identify single nucleotide polymorphisms (SNPs) within the 5'UTR of Bcl-2 mRNA that affects p53-dependant RNA degradation and Bcl-2 expression. We sequenced the highly conserved P2 region in 200 individuals from the Lovelace Smokers Cohort (LSC) and were unable to identify single nucleotide polymorphisms within this highly conserved region. Because p53 has a single nucleotide polymorphism (SNP) at codon 72 (rs1042522) that modifies the common amino acid, arginine encoded by CGC, to a proline encoded by CCC, we next tested the idea whether the two p53 variants affect the interaction with 5'UTR sequences within *bcl-2* mRNA. The Pro at codon 72 constitutes the second of the five PXXP (where P indicates proline and X indicates any amino acid) within the proline-rich domain (aa 61–94)[32,33] and two independent cohort studies had found that the p53^{Pro} variant is associated with attenuated decline in lung function in humans[34,35]. Because of the finding that p53 is a critical regulator of *bcl-2* mRNA and the resolution of MCM we tested whether polymorphisms within p53 may be associated with CMH in the LSC.

Initially, we genotyped participants of the LSC when only 1102 women were enrolled of whom 370 participants had CMH as defined by having self-reported cough and productive

phlegm for 3 months a year for at least 2 consecutive years[36] and 732 did not. Of the 1102 women, 77 (7%) were homozygous $p53^{Pro}$, 606 (55%) homozygous $p53^{Arg}$, and 419 (38%) heterozygous $p53^{Arg/Pro}$. We found that after adjusting for age and smoking duration, subjects who are homozygous for the rare $p53^{Pro}$ allele had a significantly reduced odds for chronic bronchitis compared to those with the $p53^{Arg}$ genotype (OR=0.48, p=0.03).

The p53 PRD is important for interaction with *bcl-2* mRNA

To investigate whether the p53 SNP affects *bcl-2* mRNA half-life and to possibly identify the domain in p53 that interacts and destabilizes *bcl-2* mRNA, we compared *bcl-2* mRNA levels and half-lives in three HAECs individually each homozygous for the $p53^{Arg}$ and $p53^{Pro}$ variants. We found that after averaging the *bcl-2* mRNA levels in HAECs with the $p53^{Arg}$ variant ($HAEC^{Arg}$) were approximately 2-fold greater than in $p53^{Pro}$ HAECs (Fig. 3A). *Bcl-2* mRNA half-life was >10 h in primary HAECs, irrespective of genotype, when p53 was not activated but following activation of p53 by irradiating these cells to 10 mJ UV light, *bcl-2* mRNA half-life was reduced to 1.2 h in $HAEC^{Pro}$ and to 7 h in $HAEC^{Arg}$ cells (Fig. 3B). This reduction in *bcl-2* mRNA half-life by $p53^{Pro}$ suggests that the PRD of p53 plays an important role in this decay process. Bcl-2 protein levels were also reduced in $HAEC^{Pro}$ compared to $HAEC^{Arg}$ cells (Fig. 3C).

To test whether the $HAEC^{Pro}$ would also express less mucus compared to $HAEC^{Arg}$ cells, we identified 10 HAEC each from individuals homozygous for $p53^{Pro}$ and $p53^{Arg}$ and differentiated them individually in culture over 21 d at air-liquid-interface (ALI) on Transwell membranes. When averaged, MUC5AC mRNA levels in these cultures were significantly lower in $HAEC^{Pro}$ compared to $HAEC^{Arg}$ (Fig. 3D). In addition, $HAEC^{Pro}$ cultures exhibited less secreted mucus (Fig. 3E) and mucous cells per mm basal lamina compared to $HAEC^{Arg}$ cultures (Fig. 3F). These results showed that the $p53^{Pro}$ and $p53^{Arg}$ genotypes affected the mucous phenotype.

The polymorphism at codon 72 affects the mucous regulatory network

In airway epithelial cells, increased survival per se is not sufficient to provide the mucous differentiation phenotype, suggesting that $p53^{Arg}$ may be controlling genes that affect the mucous differentiation pathway. Therefore, we isolated RNA from 10 each differentiated $HAEC^{Pro}$ and $HAEC^{Arg}$ cultures and interrogated all expressed genes by microarray analysis. One of the genes found to be expressed at significantly lower levels in $HAEC^{Pro}$ compared to $HAEC^{Arg}$ cultures was SPDEF. From the list of genes identified to be differentially expressed, we focused on SPDEF, because it has recently been described as being a transcription factor sufficient to cause goblet cell differentiation of Clara cells[37] and as a regulator of the transcriptional network mediating the goblet cell differentiation and mucus hyperproduction associated with chronic pulmonary disorders[38]. Differences in expressed genes were validated using qRT-PCR and showed that expression of MUC5AC, MUC5B, and SPDEF were reduced in $HAEC^{Pro}$ compared to $HAEC^{Arg}$ cultures (Fig. 3G). In addition, using adenoviral expression vectors forced expression of $p53^{Pro}$ in $HAEC^{Arg}$ cultures from 3 individuals significantly reduced expression of MUC5AC, MUC5B, and SPDEF mRNAs (Fig. 3H) while expression of $p53^{Arg}$ in $HAEC^{Pro}$ cultures from 3 individuals increased expression of these genes reversing the endogenous levels of these

mRNAs (Fig. 3I). In addition, suppression of Bcl-2 or SPDEF using retroviral shRNA vectors reduced MUC5AC mRNA levels in HAEC^{Arg} cultures (Supplementary Fig. 4A, B, C, D). These findings further demonstrated that it is the genotype of p53 that determined expression of genes driving the mucous regulatory phenotype.

While Bcl-2 may sustain hyperplastic mucous cells, we assumed that SPDEF may be responsible for the differentiation of the HAEC^{Arg} cultures to express the mucous phenotype. Therefore, we investigated whether the promoter region of SPDEF may be driven differently by two p53 variants to cause the observed differences in mucous differentiation of HAECs. We identified two putative p53 response elements within 1 kb upstream of the SPDEF transcriptional start site and cloned this region into pGL3 Basic containing a luciferase reporter and tested activation in H1299^{ts}Arg and H1299^{ts}Pro cells. Following transfection with the luciferase construct and activation of the temperature-sensitive p53 by shifting cells from 37° to 32°C for 18 h, the SPDEF promoter activity was consistently 2-fold lower in p53^{Pro} versus p53^{Arg} cells (Fig. 3J). These findings suggested that p53^{Arg} has a higher affinity to the SPDEF promoter. Therefore, we performed chromatin immunoprecipitation (ChIP) assays using p53 antibodies and found that the 0.3 kB region of the SPDEF promoter was recovered at significantly higher levels from H1299^{ts}Arg compared to H1299^{ts}Pro cells (Fig. 3K). The 4 kB upstream region was used as a negative control and showed little interaction in both cell lines (Fig. 3L). These findings confirmed that p53-SPDEF promoter binding exhibited a significantly higher affinity in H1299^{ts}Arg versus H1299^{ts}Pro cells.

The p53 response element is defined by two canonical decamers separated by a spacer of 0–13 nucleotides[39]. The SPDEF promoter region contained two (RRRCWWGYYY) motifs with a four nucleotide spacer. Because the core region (CWWG) is critically important for p53 binding[39], deletion mutations were generated by removing six nucleotides for each of the two motifs in the core region to form two different 6 NT deletions termed Mut11 and Mut21. The empty plasmid, Mut11, and Mut21 constructs when tested in the parental H1299, H1299^{ts}Arg, and H1299^{ts}Pro cell lines showed that while p53^{Arg} is better than p53^{Pro} in activating the wild-type promoter, SPDEF promoter activity was significantly reduced in both Arg and Pro cell lines when the core regions of the p53 response elements were absent (Fig. 3K). These findings confirmed that p53 activated SPDEF promoter by interacting with these conserved response elements.

Susceptibility to death in cells harboring p53^{Arg} or p53^{Pro}

Bcl-2 suppresses DNA damage-induced cell death[40]. Because p53^{Pro} drastically reduced *bcl-2* mRNA stability, we investigated whether cell death is enhanced in p53^{Pro}-expressing cells that are grown in the presence of mRNA synthesis inhibitors and various cell death stimuli. When treated with the DNA damaging agent, doxorubicin (Dox), H1299p53^{ts}Pro cells were more sensitive to the DNA damage-than H1299p53^{ts}Arg cells, but not to cycloheximide (CHX)- or thapsigargin (TG)-induced cell death (Fig. 4A).

In mice, the PRD consists of two PXXP motifs highly resembling human p53. Mice expressing p53 lacking the four critical proline residues at loci 79, 82, 84, and 87 that make up the tandem PXXP sites (p53^{AXXA}) were generated to study the role of the PRD in

Mdm2-mediated degradation of p53[41,42]. The p53^{AXXA} mice develop normally and the transcriptional activation of target genes, apoptosis induction[42], or acetylation[43] is not impaired. MEFs from p53^{WT} and p53^{AXXA} mice showed comparable rate of proliferation in culture. We first subjected cultured MEF cells to UV light and determined that the mutation of the PXXP motif to AXXA of the PRD does not prevent stabilization of p53 protein by Western blotting (Fig 4B). Analysis of the dying cells revealed that when treated with Dox the MEF^{WT} compared with MEF^{AXXA} cells showed a higher percentage of Annexin V-and PI-positive cells at 8 h (Fig. 4C). MEFs from p53^{wt} mice were more susceptible to Dox-, UV irradiation-, hypoxia-, or hyperoxia-induced cell death than p53^{AXXA} MEFs, especially in the presence of the transcription inhibitor, DRB at 8 h (Fig. 4D) and at 18 h (Supplementary Fig. 6A, B) after treatment with cell death inducers. However, MEFs were equally sensitive to thapsigargin (TG)- (Fig. 4D) or cycloheximide (CHX)-induced cell death (Fig. 4D and Supplementary Fig. 6). These findings suggest that when transcription is blocked, enhanced degradation of *bcl-2* mRNA by the p53^{Pro} variant makes cells more susceptible to DNA damage-induced cell death compared to cells in which the PRD is modified resulting in a longer half-life and higher *bcl-2* mRNA levels. This was also true in the absence of the transcriptional inhibitor where in p53^{AXXA} MEFs cell death was significantly reduced compared to p53^{wt} MEFs. Further, p53^{wt} and p53^{AXXA} MEFs were infected with adenoviral vectors expressing p53^{Arg} and p53^{Pro} and then treated with Dox. Western blotting following infection with Ad-p53^{Arg} and Ad-p53^{Pro} showed that similar levels were expressed (Fig 4E). However, cell death in MEFs was significantly increased when infected with Ad-p53^{Pro} and, as expected, p53^{wt} MEFs gained resistance to cell death when infected with Ad-p53^{Arg} (Fig. 4F). These findings further confirm that the p53^{Pro} variant enhances decay of the anti-apoptotic Bcl-2 and thereby sensitizes cells to Dox-induced cell death.

PRD of murine p53 also affects the mucous regulatory network

To determine whether the two PXXP motifs or the two threonines affect mRNA stability, we compared *bcl-2* mRNA stability in MAECs and MEFs from wild-type p53 (p53^{wt}), p53^{AXXA}, and p53$^{\Delta P}$ mice. *Bcl-2* mRNA levels were higher in mutant alleles versus wild-type in MEFs (Fig. 5A) and MAECs (Fig. 5D) and mRNA half-life was increased from 1.5 to ~5 h in MEFs (Fig. 5B and Supplementary Fig. 2I) and 2 to ~4 h in MAECs (Fig. 5E and Supplementary Fig. 2J) from p53^{wt} and p53^{AXXA} mice, respectively, following activation of p53 with 10 mJ UV radiation. Bcl-2 protein levels were also increased in MEFs (Fig. 5C) and MAECs (Fig. 5F) from p53^{AXXA} compared to p53^{WT} mice. These results confirm that the murine p53 PRD, similar to the human p53 PRD, is crucial in affecting *bcl-2* mRNA decay. Furthermore, the studies in murine cells show that modifying not only the prolines but also the threonines within the p53 PRD to alanines equally increased *bcl-2* mRNA levels.

Because mucus levels increase in those individuals harboring the p53^{Arg} variant, we investigated whether changes in murine PRD also affect expression of the mucus regulatory network. Mice with a deletion of the PRD (p53$^{\Delta P}$) or expressing p53 lacking the four critical proline residues at loci 79, 82, 84, and 87 that make up the tandem PXXP sites (p53^{AXXA}) were generated to study the role of the PRD in Mdm2-mediated degradation of p53[41,42].

MAECs isolated from wild type, $p53^{AXXA}$, and $p53^{\Delta P}$ mice and differentiated on air-liquid-interface (ALI) cultures showed increased levels in SPDEF, Muc5ac, Muc5b, and mRNAs compared to the $p53^{wt}$ MAECs (Fig. 5G). Because MEFs express comparable levels of SPDEF transcripts as MAECs (Supplementary Fig. 6C), we conducted a ChIP assay to determine whether similar to the human cells p53 may interact with the murine SPDEF promoter region. A 0.7 kB region of the murine SPDEF promoter was recovered at significantly higher levels from $p53^{AXXA}$ compared to $p53^{WT}$ MEFs (Fig. 5H). A 6 kB upstream region was used as a negative control and showed no interaction in $p53^{AXXA}$ and $p53^{WT}$ MEFs (Fig. 5H). These findings confirmed that the murine SPDEF promoter also interacts with p53 and that replacing the prolines with alanines significantly increased affinity to the promoter region.

Further, we infected MAECs from $p53^{AXXA}$ and $p53^{\Delta P}$ mice with adenoviral expression vector for GFP (Ad-GFP) or $p53^{Pro}$ (Ad-$p53^{Pro}$) to test whether the $p53^{Pro}$ is protective from increased mucus production. Cells were allowed to differentiate in ALI cultures and analyzed for SPDEF, Muc5ac, and Muc5b mRNAs levels. Levels of these mRNAs were reduced when these cells were infected with Ad-$p53^{Pro}$ versus Ad-GFP (Fig. 5I). These findings further define the role of $p53^{Pro}$ variant as being protective from increased mucous production.

Another mouse strain in which threonines 76 and 86 were mutated to alanines ($p53^{TTAA}$) was generated to remove putative Pin1 binding sites[42]. Because modification of the PRD within p53 appeared to modify the regulation of SPDEF and Bcl-2 and the human epidemiological data indicated that the p53 variants was associated with CB, we investigated expression of Muc5ac and Muc5b in the lung tissues not only of $p53^{wt}$, $p53^{AXXA}$, and $p53^{\Delta P}$ mice but also of $p53^{TTAA}$ mice. Consistent with findings in human studies, increased Muc5b (Fig. 6A) and Muc5ac (Fig. 6B) mRNA levels were more pronounced in mice with mutations in the PRD compared to wild-type mice.

To test whether this effect is observed in the C57Bl/6 background that is considered most resistant to developing mucous cell metaplasia, we backcrossed the $p53^{TTAA}$, $p53^{\Delta P}$ and $p53^{AXXA}$ mice that were generated on the 129J background into C57Bl/6 background over at least 10 generations. Results showed that in 129J and C57Bl/6 mice the mutations in the p53 PRD also increased the number of mucous cells per mm basal lamina (Fig. 6C), that this genotype drives mucous differentiation irrespective of the more resistant genetic pool present in C57Bl/6 mice. In addition, immunostaining with Muc5ac antibodies showed that tissue sections from $p53^{AXXA}$, $p53^{TTAA}$, and $p53^{\Delta P}$ mice compared with $p53^{wt}$ exhibited significantly more positivity for Muc5ac (Fig. 6D). Further, Bcl-2 and Muc5ac-positive cells in $p53^{AXXA}$ compared to $p53^{WT}$ mice are higher at 12 d after LPS instillation (Fig. 6E). While the total cell number per mm basal lamina is similar in $p53^{WT}$ and $p53^{AXXA}$ 12 d after LPS challenge the hyperplastic changes remain in $p53^{AXXA}$ but not $p53^{WT}$ mice (Fig. 6F). These findings suggest and show that the p53 PRD is central in regulating mucous metaplastic changes at baseline and during the resolution of hyperplastic changes.

Discussion

The present study defines the PRD of p53 as a crucial region that affects regulation of SPDEF and Bcl-2 to drive the mucous hypersecretory phenotype in humans and in rodents. Within the PRD of p53, substitution of Pro in the PVAP motif to Arg or Ala or modification of Thr to Ala was sufficient to increase both SPDEF promoter activity and *bcl-2* mRNA half-life and drive the mucous regulatory network at baseline and to sustain the mucous cells following a hyperplastic response.

It is generally believed that under physiological conditions, apoptosis induction by p53 mainly depends on the transcription of a distinct set of cell death regulatory genes. p53 is a major transcription factor that affects numerous promoter regions[44]. The DNA-binding region of p53 is the main region to affect transcription of genes known to directly execute apoptosis including the TNF-R family members, such as CD95/Fas/Apo-1, DR4, DR5/TRAIL-R1, and the Bcl-2 family members, such as Bax, Puma, Noxa, and Bid[45]. However, the present studies show that the PRD of p53 also enhances cell death by reducing *bcl-2* mRNA half-life through interactions with the 5'UTR region and suppressing expression of this central inhibitor of apoptosis.

Despite the previous reports that interaction of p53 with the P2 promoter region suppresses P2 promoter activity in primary airway and lung cancer cell lines[9,13], we first suspected that p53 does not suppress *bcl-2* promoter activity when we noticed that within the context of the full-length P1-M-P2 promoter. First, the extent of this suppression was not sufficient to explain the drastic reduction in Bcl-2 protein when p53 is activated and the P2 promoter region was able to suppress the P1-M promoter activity independently of p53. These observations led us to hypothesize that p53 affects *bcl-2* mRNA stability instead. We found that P2 sequences are part of the 5'UTR of *bcl-2* transcripts, which is consistent with previous studies reporting that P2 initiates a small percentage of transcripts in cells such as B cells[46]. Because of their extremely labile nature, as evidenced by the smears observed in Northern blot analyses[11,12,46], previous attempts to characterize all the *bcl-2* mRNA transcripts by techniques such as the S1 nuclease assay may not have been sufficiently sensitive. Although we also found the previously identified T2, a transcriptional start site located within the GC-rich region at −1313[11], the other transcriptional start sites, T1, T3, and T4 have previously not been reported. All these transcripts contain a region of P2 that affects mRNA stability.

The p53 interaction with the 5'UTR of *bcl-2* mRNA was demonstrated by the following studies: 1) All four *bcl-2* transcripts were precipitated from cell extracts with p53 antibodies; 2) p53 was detected in pull-down assays using *in vitro* synthesized *bcl-2* mRNA; 3) $p53^{Pro}$ more drastically than $p53^{Arg}$ destabilized endogenous *bcl-2* mRNA and luciferase mRNA that was expressed from the P1-M-P2 luciferase constructs; and 4) Deletion or mutations of a 16 nucleotide region of P2 prolonged the luciferase mRNA half-life, demonstrating that p53 reduces *bcl-2* mRNA half-life by interacting with this 16 nucleotide region within the 5'UTR. Previous studies have found that the AU-rich elements (AREs) in the 3'UTR of *bcl-2* mRNA can bind AUF1 and TINO that cause a 2–fold destabilization of the mRNA[47,48] or Bcl-2 protein itself that is required for ARE-dependent degradation of its own

mRNA[47]. Nucleolin, another protein that interacts with the AREs, stabilizes the *bcl-2* mRNA[49].

The p53-mediated decay required only the 5'UTR but is independent of the 3'UTR of *bcl-2* mRNA. The $p53^{Pro}$ variant may be more efficient than the $p53^{Arg}$ variant in forming a macromolecular complex that helps recruit RNA enzymes to target *bcl-2* mRNA. We searched both the genome and transcriptome for exact matches to the 16 nucleotides that were important for the interaction and enhanced decay of *bcl-2* mRNA. Two other exact matches were found in the genome, and both reside approximately 37.5kb away from the FRG2 and FRG2B genes on chromosomes 4 and 10, respectively, but neither of these positions are transcribed regions. No exact matches, other than in the *bcl-2* 5' UTR, were found in a search of all RefSeq and GenBank mRNAs. Mutation of 4 nucleotides on either end of the 16 nucleotides did not fully stabilize the *bcl-2* mRNA although these changes abolished interaction of p53 from cell extracts. These findings suggest that secondary structures of the *bcl-2* mRNA rather than a specific nucleotide sequence may be important for interaction with p53. The participation of factors that may bind to P2 sequences and form a scaffold for p53 interaction are yet to be identified. One previous study has reported that p53 binds to the 5' UTR of cdk4 to inhibit TGF-beta-regulated translational of cdk4[50].

The similar half-life of *bcl-2* mRNA in HAECs and p53-deficient H1299 cells suggests that the function of p53 to enhance decay is tightly regulated. In addition, the need to activate p53 by UV irradiation in order to reduce *bcl-2* mRNA half-life in HAECs implies that either only activated p53 can interact with *bcl-2* mRNA or that other factors may facilitate this interaction. A wide range of cellular stresses, such as DNA damage, telomere erosion, aberrant oncogene activation, or hypoxia cause p53 accumulation and activation, indicating that protein abundance may dictate function[10]. The observation that *bcl-2* mRNA half-life in A549 cells was reduced without inducing a cellular stress response supports that p53 is either constitutively activated in these cells in regard to destabilizing *bcl-2* mRNA or that the factor(s) required for p53 interaction with *bcl-2* mRNA are present. However, because p53 levels are low in A549 cells, we speculate that post-translational modifications such as phosphorylation of various serine and threonine residues, acetylation, and methylation of specific p53 domains[51] and/or cooperation with other transcription factors[52] may be responsible for the interaction to enhance the decay of *bcl-2* mRNA.

Modifying p53 expression in both SAOS-2 and HCT116 cells or simply substituting the proline or threonine residues within the PRD of p53 affected *bcl-2* mRNA levels and mRNA half-life in human and murine cells. The fact that it is not only the substitution of the conserved PXXP motif but also the substitution of threonines with alanines affecting the decay of *bcl-2* mRNA across cell types and species suggests that it is the conformational change that is introduced by any modification within the PRD to be the primary cause for the ability of p53 to interact with higher affinity to SPDEF promoter or *bcl-2* mRNA. The PRD lies within the N-terminal region of p53 (aa 61–94) and is characterized by two transactivation domains (TAD) that are required for transcriptional activation of target genes[51]. Previous studies have focused on the contribution of the PRD to the regulation of p53 stability, transactivation ability, and induction of transcription-independent apoptosis[32,33,53]. $p53^{Pro}$ activates expression of certain genes by binding more strongly to

TAFII70 and TAFII32, major components of the basic transcriptional machinery, than does $p53^{Arg33}$. That $p53^{Arg}$ compared to $p53^{Pro}$ interacts stronger with both the P2 sequences of the *bcl-2* mRNA and the SPDEF promoter is consistent with those observations. Consistent with our findings, a previous study had reported that Bcl-2 immunopositivity tended to be more in tumors with the $p53^{Arg}$ variant[54]. However, the present studies are the first to link the PRD of p53 to regulating mRNA stability.

At baseline, $p53^{AXXA}$ mice show increased metaplastic mucous cells compared to $p53^{WT}$ mice while the total airway epithelial cell numbers are similar, likely due to increased SPDEF levels. However, after LPS instillation that caused a hyperplastic response equally in $p53^{+/+}$ and $p53^{-/-}$ mice, the resolution of hyperplasia was intact in $p53^{+/+}$ mice but was disrupted in $p53^{-/-}$ and $p53^{AXXA}$ mice. The induction of mucous expression in mice instilled with LPS is independent of SPDEF, as during such inflammatory responses IL-1β[55] and neutrophil elastase[56] cause increased expression of Muc5ac and Bcl-2[57]. However, sustained hyperplasia in $p53^{-/-}$ and $p53^{AXXA}$ mice is likely due to increased Bcl-2 expression in these mice.

When transcription is blocked with 5,6-dichloro-1-beta-D-ribobenzimidazole (DRB), $p53^{Pro}$ more efficiently causes cell death than $p53^{Arg}$ due to drastically reduced Bcl-2 levels caused by the high *bcl-2* mRNA decay rate by $p53^{Pro}$. The finding that cyclohexamide- or thapsigargin-induced cell death equally well in both H1299$p53^{ts}$Arg and H1299$p53^{ts}$Pro cells when co-treated with DRB may suggest that Bcl-2 does not affect protein shutdown- or ER-induced cell death but DNA damage-induced cell death caused by doxorubicin, UV irradiation, hyperoxia, or hypoxia. Cell type differences in apoptotic pathways induced by $p53^{Arg}$ and $p53^{Pro}$ may explain the findings that the $p53^{Pro}$ was found to be less apoptotic[58]. Findings from our studies suggest that using a combination of DNA polymerase II inhibitors to enhance *bcl-2* mRNA decay along with radiation and chemotherapy may better target cancers of individuals harboring the $p53^{Arg}$ genotype rather than using DNA damaging agents only. While the association of the p53 polymorphisms with cancer incidence is inconclusive, several studies have suggested that individuals homozygote for $p53^{Arg}$ have a better response and survival rate following chemo- and radiation therapy for head and neck, breast, and lung cancers (reviewed in[59]).

The effect of this SNP on the mucous differentiation pathway is highly conserved, suggesting that these mice with modifications in the PRD of p53 closely reflect the susceptibility in humans and should be most appropriate for screening potential drugs to treat chronic mucous hypersecretion. Many drugs that are screened in mice fail in human trials because of vast differences in pathways. Testing potential drugs in mice that replicate the disease in humans, such as the $p53^{AXXA}$ mice, not only would help in improve design but also increase the likelihood of success in human clinical trials. Similar strategies that use genetically engineered mouse models have shown success in predicting the outcome of clinical trials[60,61].

Materials and Methods

Study Population

The LSC (Lovelace Smokers' Cohort) is a well-characterized cohort of current and former smokers in New Mexico. Recruitment, inclusion, and exclusion criteria have been described previously[62,63]. Briefly, study subjects were drawn from a cohort study Albuquerque, NM and its surrounding communities. Most participants were recruited through newspaper or television advertisements and were paid a small stipend for their participation. Subjects were included in the study if they were ages 40 to 75 years, former or current smokers with a minimum smoking history of 20 pack-years on initial screening, and able to understand English. Information related to demographics, respiratory diseases, and smoking was obtained by self-report from all study participants via a questionnaire. Spirometry was obtained on all subjects by certified and registered respiratory therapists strictly adhering to the 1994 American Thoracic Society (ATS) guidelines. The LSC disproportionately enrolled women ever-smokers since the disease prevalence from 1998 onwards is significantly higher among women than men[64] and since women are underrepresented in most COPD studies in the United States[65]. This study is approved by the Western Institutional Review Board (Olympia, WA; #20031684) and all subjects sign informed consent for their participation.

Animals

Pathogen-free wild-type 129J and C57BL/6J mice and $p53^{-/+}$ breeders were purchased from The Jackson Laboratory (Ben Harbor, ME). $p53^{wt}$, $p53^{AXXA}$, $p53^{TTAA}$, and $p53^{\Delta P}$ mice on 129J background were provided by Dr. Geoffrey M. Wahl (Salk Institute for Biological Studies, LaJolla, California). Mice were housed in isolated cages under specific pathogen-free conditions and bred at LRRI for the described studies. The $p53^{\Delta P}$ mice were genotyped by standard PCR that show different products from wild-type mice and the AXXA and TTAA mice were genotyped using restriction digestion of PCR amplified products to distinguish the knock-in from wild-type mice (primer sequences can be found in Supplementary Table 3). These mice were also backcrossed for at least 10 generation into the C57BL6 background. Right cranial lung lobes were removed from mice and tissue homogenized using TissueLyser II (Retsch, Newtown, PA) and RNA isolated and qRT-PCR performed as described previously[29]. Mice were randomized by weight for each study. $p53^{+/+}$ and $p53^{-/-}$ mice were intransally instilled with 60 μg LPS as described[29]. Left lungs were inflated and fixed at 25 mm pressure with zinc formalin for preparing tissue sections which were stained with Alcian blue (AB), hematoxylin (H) and eosin (E) or were immunostained. Images were captured using NanoZoomer Digital Pathology slide scanner (Hamamatsu, Bridgewater, NJ) and epithelial and mucus cells quantified using Visiopharm Integration System (VIS) software (Horsholm, Denmark). For all mice, epithelial cells in the axial airway of the left lung at generation 4 or 5 are quantified. A minimum of 3 adult mice were used for isolation of MAECs that were cultured for differentiation on Transwell inserts according to described methods[66]. All experiments were approved by the Institutional Animal Care and Use Committee of Lovelace Respiratory Research Institute (LRRI) and were conducted at LRRI, a facility approved by the Association for the Assessment and Accreditation for Laboratory Animal Care International.

Cells

Primary human airway epithelial cells (HAECs) from individuals homozygous for the $p53^{Arg}$ and $p53^{Pro}$ variants were obtained from lungs under the protocol and consent form approved by the University of North Carolina School of Medicine Committee on the Protection of the Rights of Human Subjects. HAECs from each individual and those purchased from Clontech (Walkersville, HD), and AALEB cells (Immortalized and transformed human airway epithelial cells)[67] were maintained in BGEM media (Cambrex Biosciences, Walkersville, HD) with various supplements as described[68]. After seeding primary HAECs on Transwell membranes and differentiating them on air-liquid interface, membrane quarters were used for qRT-PCR and membrane halves embedded in paraffin. Sections were stained with AB/H&E and imaged with Nikon (Irvine, CA) E600 light microscope and 40X images captured with Nikon DXM1200F camera using ACT-1 software. Epithelial and mucus cells quantified using Visiopharm Integration System (VIS) software.

SAOS-2 (human osteosarcoma cell line, ATCC HTB-85), Calu-3 (human lung Adenocarcinoma cell line, ATCC HTB-55), H23 (NCI-H23, lung Adenocarcinoma, ATCC CRL-5800), HBEC-2 (human immortalized airway epithelial cells), and A549 (Immortalized and transformed human alveolar cells, ATCC CCL-185) cells were maintained in Dulbecco's modified Eagle's media (DMEM) supplemented with 10% FBS. Expression vectors for $p53^{Arg}$ or $p53^{Pro}$ variants at codon 72 have been shown to induce cell death differentially in SAOS-2 cells[58]. The H1299 cell line (NCI-H1299, ATCC CRL-5803), a p53-deficient cell line that is derived from a non-small cell lung cancer, was used to generate stable cell lines by transfecting with pCMV-neo-bam $tsp53^{Arg72}$ or pCMV-neo-bam $tsp53^{Pro72}$ plasmids (gift from Dr. Murphy, University of Pennsylvania, PA) that express temperature-sensitive p53 variants. These variants are essentially inactive at 37°C but are activated when cells are shifted to 32°C. Clones expressing similar p53 protein levels were selected for further experiments (see Supplementary Fig. 5). H1299 cells and those harboring temperature-sensitive p53 variants for Arg and Pro at codon 72 were maintained in RPMI-40 (Gibco) with 10% FBS, and 2 mM glutamine, and 400 μg/ml G418 (Sigma Chemicals).

Mouse embryonic fibroblasts (MEFs) from $p53^{wt}$, $p53^{\Delta P}$, $p53^{TTAA}$, and $p53^{AXXA}$ mice were derived from day 14.5–16 embryos, and were cultured in DMEM supplemented with 10% FBS and were used for experiments at passages 3–8. MEFs were infected (10 MOI) with adenoviruses expressing $p53^{Arg}$ or $p53^{Pro}$. Twenty-four hours later, cells were washed and treated with 1 μM doxorubicin for 24 h. Cells were counted and harvested for western blot analyses. SAOS-2 cells stably transfected with either p53-expressing plasmid (SAOSp53) or vector only (SAOS-2Ctr) were a gift from Dr. Michael Resnick (National Institute of Health Environmental Sciences; Dallas, TX), and were maintained in DMEM supplemented with 10% FBS and 0.5 mg/ml G418.

Cell Death Assay

Following treatment with 50 ng/ml DRB and either 1μM doxorubicin, 10 μM cyclohexamide, or 1 μM thapsigargin, viable cell numbers were quantified using trypan blue

exclusion method. Cells were also irradiated with 10 mJ UV light, were treated with hypoxia (5% O_2/95% nitrogen) or hyperoxia (95% O_2/5% nitrogen) for 30 m at room temperature and were cultured in 37°C incubator with 5% CO_2/ 95% air. Cells were harvested 24 h after treatment by trypsinization and cell numbers were quantified using trypan blue exclusion method. For AnnexinV-PI staining, approximately ~ 10^5 cells were also stained in 1X binding buffer (0.01 M HEPES, pH 7.4; 0.14 M NaCl; 0.25 mM $CaCl_2$) using 5 l propidium iodide (Sigma) and 10 μl of Annexin V-FITC (BD PharMingen). The reaction was incubated in the dark for 15 min at room temperature and the percentage of FITC- and PI-positive cells were collected on FACS Canto (BD Biosciences; San Jose, CA) flow cytometer and analyzed using FlowJo software (ver 7.6.3; TreeStar, San Carlos, CA).

Generation of Deletion Constructs and Site-Directed Mutagenesis

The generation of the P1-M-P2 luciferase construct has been described previously[13] and the P1-M-P2 constructs in which P2 was serially deleted (P1-M-P2Δ1–10) were generated by amplifying the P2 region with primers listed in Supplementary Table 1 that introduced the upstream Bgl-II and a downstream Hind-III site. The amplified products were then used to replace the full-length P2 sequence that was removed by restriction digestion using Bgl-II and Hind III. For *in vitro* mRNA synthesis, the P1-P2Δ10 luciferase construct was cloned in to PCRIITOPO vector (Invitrogen) that has the dual promoter system for REMSA.

The 50-nucleotide-long forward and their reverse oligonucleotides sets were designed having the Xba-I in the upstream sequence and Hind-III restriction site on the downstream sequence. The 16-nucleotide sequences with putative p53-interaction sites were mutated by changing the purines to pyrimidines as shown by the underlined sequences in Supplementary Table 2. The oligonucleotides were annealed, double-stranded DNA generated, and following digestion with Xba-I and Hind-III restriction fragments were cloned into a pCR-II dual promoter vector. These plasmids were then used for *in vitro* transcription (IVT) and pull-down using 1:500 diluted p53 antibody (sc-98, Santa Cruz Biotechnology, CA).

Two deletion mutants were generated in the dual promoter vector, pCR-2.1, harboring the P2 region using Quickchange site-directed mutagenesis kit (Stratagene) according to manufacturer's protocol. The resulting mutant constructs, pCR-2.1 P2(−482/−468) and PCR-2.1 P2(−443/−429), in which 16 and 14 nucleotides, respectively, had been deleted were used for IVT synthesis and pull-downs using the p53 antibody (sc-98, Santa Cruz). The P1MP2Δ(−443/−429) luciferase construct in which 16 nucleotides were deleted from P1MP2 luciferase plasmid and PIMP2Δ(−443/−439 and −433/−429) were generated at Mutagenex Inc. (Somerset, NJ). These deleted plasmids were used for transient transfection in HCT116 p53 positive cells to determine the effect of this deletion on luciferase mRNA half-life. Both SPDEF promoter deletion mutants (Mut11 and Mut21) were also generated at Mutagenex.

RNA Extraction and RT-PCR

Total RNA was extracted from Calu-3, A549, AALEB, SAOS-2, H1299, HBEC-2, NHBEC, and transfected H1299 cells using TRI reagent (TR-118; Molecular Research Centre, Inc.)

as described by the manufacturer. For cDNA synthesis, 1μg of total RNA or RNA treated with RNAse free DNase (Invitrogen) were reverse-transcribed with Random Hexamers (Promega). Primers with the following sequences: M Forward: 5'-GCAGGACCAFFAGGAGGAGA-3', M Reverse 5' GGTGG GGGAGG TTTTATTT-3', and P2 Forward: 5'- CGATC TGGAA ATCCT CCTAATT -3' and P2 Reverse: 5'TTGGCATGAGATGCAGGAAA-3 were designed to amplify the M and P2 regions of the *bcl-2* promoter. After denaturing at 95°C for 5 min, reactions were amplified for 35 cycles using annealing temperatures of 55°C for M primers and 60°C for P2 primers.

5'Rapid Amplification of cDNA Ends (RACE)

To identify the 5'UTR, we used the rapid amplification of cDNA ends (RACE) kit (Invitrogen; San Diego, CA) on RNA isolated from HAECs according to the manufacturer's instructions. Briefly, total RNA (5 μg) was dephosphorylated with 10 U/μl calf intestinal phosphatase (CIP) and treated with 0.5U/μl tobacco acid phosphatase (TAP) to removes the 5' CAP structure. The 5'gene racer oligo was ligated to the RNA using T4 RNA ligase and the first strand cDNA was synthesized using random hexamers and superscript III RT. Transcripts were identified by PCR using the gene racer primer R1 and primers specific to the M region (M1: 5'GTGGGGGAGGTTTTATTT-3') or *bcl-2* open reading frame (ORF1: 5'CGCTGGGAGAACAGGGTACGATAA -3'). Amplification using nested racer primer R2 and gene-specific primers specific to the M region (M2: 5'-ATGACTGCTACGAAGTTCTCCC-3') and the *bcl-2* open-reading frame (ORF2: 5'-TGGCGCACGCTGGGAGAACA-3) were used to ensure specificity of products, followed by cloning into TOP10 vector (Invitrogen, CA) for sequencing.

mRNA Half-Life Studies

Following treatment with the transcription inhibitor 5,6-dichloro-1-beta-D-ribobenzimidazole (DRB) (Sigma-Aldrich) total RNA was extracted using TRIzol reagent. RNA levels were normalized using 18S rRNA and GAPDH amplified from the same RNA samples using Pre-Developed 18S rRNA (VIC-MGM) and hGAPDH (ABI Assay-on-Demand FAM-MGM probe). Relative mRNA abundance was calculated using the ΔΔCt method and mRNA half-life was calculated as described[43]. The primers and probe for detecting luciferase mRNA expression by qRT-PCR were LUCForward-ACCTCCGTACTATCCTTTGGAAGAA LUCReverse-GGAACTGCGGCATATCGTGATA and the probe sequence with the dye LUC-FAM-ACTGCGGGAGAACAA.

Western Blot Analysis

Cell extracts were prepared using RIPA buffer (20mM Tris, pH 7.4, 137 mM NaCl, 1% NP-40, 0.25% Deoxycholate, 0.1% SDS, 1mM EDTA and 1% protease inhibitor cocktail). Protein concentration was determined by BCA kit (Pierce; Rockford, IL) and 100 μg protein was analyzed by Western blotting as described previously[69]. Anti-p53 (sc-98, Santa Cruz) was used at 1:1000 (2 μg/mL) dilution and anti-Bcl-2 (sc-492, Santa Cruz) and anti-β-actin (Sigma) were used at 1:1000 dilutions. SPDEF antibodies (gift from Dr. Jeffery Whitsett, Children's Hospital, University of Cincinnati, OH) were used at 1:5000 dilution. Proteins

were detected using ECL and visualized by chemiluminescence (Perkin Elmer, Waltham, MA) using the FujiFilm Image Reader LAS-4000 (Valhalla, NY). The uncropped scans of the most important Western blots are included as a supplementary figure in the Supplementary Information.

Co-Immunoprecipitation Assays

Immunoprecipitation of protein-RNA complexes was performed as described previously[70]. H1299p53^{ts} cells were incubated at 32°C, harvested (8×10^7), and proteins cross-linked using formaldehyde (Sigma) at a final concentration of 0.5% (v/v) and incubated at room temperature for 10 min. Cross-linking was quenched with glycine (pH 7.0, 0.25M final concentration) and cells were lysed with three rounds of sonication in 1ml of RIPA buffer containing protease inhibitors. An aliquot of the cell lysate (500μl each) was mixed with 20μl of protein-A Sepharose beads for 1 h at 4°C followed by centrifugation at 400g for 5 min. The pre-cleared supernatant was diluted with RIPA buffer (250μl) containing RNAsin and protease inhibitors, mixed with polyclonal anti-p53 (0.2 μg/μl) (sc-98, Santa-Cruz) or IgG (0.2μg/ml) and incubated overnight at 4°C with slow mixing. Protein-A Sepharose beads (100μl) were added to the samples followed by incubation at 4°C for 3 h. The Sepharose beads were washed five times with RIPA buffer, beads were centrifuged for 5 min at 200g and mRNA-protein complexes eluted with 120μl hot SDS and boiled for 5 min. Beads were incubated at 70°C for 45 min to reverse cross-linking and then centrifuged for 5 min at 13,000g and eluted. From both p53 and IgG_1, 20 μl samples were removed for Western blot analysis. RNA was extracted from the remaining samples using TRIzol (Invitrogen) according to manufacturer's protocol, treated with DNAse I, and used as a template for qRT-PCR using probe and primer set for human Bcl-2 (ABI Assay-on-Demand FAM-MGM probe) and to synthesize cDNA using random hexamer primers (OmniScript Invitrogen). PCR was performed using 5 μl of the cDNA samples using primer sets for the four transcripts: T1 Forward: 5'CCTGC CGCGG CGCCT TTAAC3' Reverse: 5'-ATGAC TGCTA CGAAG TTCTCCC-3', T2 Forward: 5'GCAGG ACCAG GAGGA GGAGA3' Reverse: 5'GGTGG GGAGG TTTTATTT-3' .T3 Forward: 5'- CGATC TGGAA ATCCT CCTAATT -3' Reverse: 5'-TTGGC ATGAG ATGCA GGAAA-3'and T4 Forward: 5'-TGGGG TGGGA GCTGG GGCGA-3' Reverse: 5'-CCCCC GTTGC TTTTCCT-3' regions of the Bcl-2 5'UTR region.

Chromatin-Immunoprecipitation (ChIP) Assay

H1299 cells harboring temperature-sensitive p53^{Arg} or p53^{Pro} variants, and MEFs from p53^{WT} and p53^{AXXA} cells were used for ChIP assays as described previously[43]. Briefly, cells were fixed with 1% formaldehyde, and the reaction was quenched using 1.25 M glycine and scraped into cold PBS containing protease inhibitors. ChIP was performed using the Magna ChIP G kit (MAGNA0002; EMD Millipore) as described by the manufacturer. Sonicated nuclear fractions were incubated with p53 antibody using mouse monoclonal (sc-98, clone Pab1801; Santa Cruz Biotechnology, Inc.) and rabbit polyclonal (sc-6324, clone FL393; Santa Cruz Biotechnology, Inc.) for human and murine p53, respectively. DNA identification was confirmed with PCR using the following primers specific for the human and murine SPDEF promoter regions: CTGATCCATCTTAGAACCCCAGCCC (forward), and GGATCCATGCCCTGACAGCTAGG (reverse); and

GGAGAGAGAACTCAGCAGTTAAG (forward) and GTGTCACCACACCTGACTATC (reverse), respectively. The 4 and 6 kb upstream for human and murine SPDEF regions, respectively used the following specific primers: CTGTGAGTGAGACAGGCAATGACCC (forward) and TTGGGACCAGAGAGGCTAGGGAC (reverse); and GTTTGACTCTCTCCTGGCTTTC (forward) and CATCTACTAC ACGCCAAGTT CC (reverse), respectively.

In-Vitro RNA Transcription (IVT) and RNA Pull-Downs

Biotinylated RNA transcripts were synthesized using the *in vitro* transcription kit from Enzo Life sciences (Farmingdale, NY) as described by the manufacturer. Briefly, reactions were performed using T7 (sense) and SP6 (antisense) promoters to synthesize P2 RNA from pCR-2.1 P2. *In vitro* transcription (IVT) reactions contained 1 μg of linearized plasmid template treated with Proteinase K (100 μg/ml) and 0.5% SDS and reaction incubated for 30 min at 50°C. After phenol/chloroform extraction, DNA was precipitated overnight by adding ethanol. DNA was resuspended in RNAase/DNAase-free water (Hyclone, Thermo Scientific, Logan, UT) and incubated with transcription reaction for 1 hr at 37°C, before treatment with RNAse-free DNAse-1 (Turbo, Enzo Life Science, Farmingdale, NY). Biotin-labeled probes were purified by precipitating with 4 M LiCl and 100% ethanol. The RNA pellet was dissolved in 2X TEN (20 mM Tris-HCL pH 8.0, 2 mM EDTA pH 8.0 and 500mM NaCl) and quantified. Cytosolic S-100 extract was prepared using H1299p53ts cells incubated at 32°C. Cells were washed twice in cold PBS and then suspended in 500 μl of buffer D (10mM Hepes (pH 8.0), 3mM $MgCl_2$, 40mM KCl, 0.1% protease inhibitor cocktail (Sigma), 0.2% NP-40 (Nonidet P40), 10% glycerol, and 1 mM DTT (dithiothreitol) and incubated on ice for 10 min. The cells were lysed with 50 bursts using a Branson sonifier 25 sonicator (Thomas Scientific). The lysate was centrifuged at 10,000g for 2 min in order to pellet nuclei, followed by centrifugation at 20,000g for 1h at 4°C to produce the cytosolic S-100 extract. IVT RNA was incubated with 300 μg of S-100 extract in 2X TENT buffer (20mM Tris-HCL pH 8.0, 2mM EDTA pH 8.0, 500mM NaCl and 0.5% v/v Triton X-100) for 30min at room temperature with gentle mixing. Pull-downs were performed in the presence of 1% Triton X-100 using Dynabeads M-280 cross-linked to steptavidin beads (Invitrogen). Each pull down reaction was incubated with 300 μg of S-100 extract and Dynabeads for 30 min at room temperature with gentle mixing. Dynabeads were settled with magnetic beads and centrifuged for 5 min at 1,000g. The RNA-protein-bead complexes were washed three times, eluted with 30 μl hot SDS and pull-down products analyzed for p53 by Western blotting. The chromosome immunoprecipitation assay (ChIP) was performed as we have described[43].

Gene Silencing in Differentiated HAECs

Differentiated HACEs were transduced with retroviral expression vectors for Bcl-2 shRNA, SPDEF shRNA and control shRNA (Origene Technologies, Inc., Rockville MD) as per manufacturer's instructions. Transwell membranes were harvested and expression of certain genes analyzed by qRT-PCR and Western blot analyses.

Statistical Analysis

Grouped results from at least three or four different sets of experiments were expressed as mean with SEM, and differences between groups were assessed for significance by Student's t test when data were available in only two groups. When data were available in more than two groups, analysis of variance (ANOVA) was used to perform pair-wise comparison. When significant main effects were detected ($P < 0.05$), Fisher least significant difference test was used to determine the differences between groups. A *P* value of 0.05 was considered to indicate statistical significance. The difference in the mean CT values from qRT-PCR amplifications between the two homozygote genotypes of HAECs was assessed with a two-sample t-test. Both, the difference and the difference plus one standard error were summarized by expressing as fold change.

Supplementary Material

Refer to Web version on PubMed Central for supplementary material.

ACKNOWLEDGEMENTS

We thank Kurt Schwalm and Lois Herrera for assistance in selected experiments and Tom Gagliano for preparation of figures. This work was supported by a grant from the National Institutes of Health (HL68111, ES015482, and HL107873).

REFERENCES

1. McCall TD, Pedone CA, Fults DW. Apoptosis suppression by somatic cell transfer of Bcl-2 promotes Sonic hedgehog-dependent medulloblastoma formation in mice. Cancer research. 2007; 67:5179–5185. [PubMed: 17545597]
2. Stathopoulos GT, et al. Epithelial NF-{kappa}B activation promotes urethane-induced lung carcinogenesis. Proc Natl Acad Sci U S A. 2007; 104:18514–18519. [PubMed: 18000061]
3. Vaux DL, Cory S, Adams JM. Bcl-2 gene promotes haemopoietic cell survival and cooperates with c-myc to immortalize pre-B cells. Nature. 1988; 335:440–442. [PubMed: 3262202]
4. Cory S, Vaux DL, Strasser A, Harris AW, Adams JM. Insights from Bcl-2 and Myc: malignancy involves abrogation of apoptosis as well as sustained proliferation. Cancer research. 1999; 59:1685s–1692s. [PubMed: 10197581]
5. Cleary M, Smith S, Sklar J. Cloning and structural analysis of cDNAs for bcl-2 and a hybrid bcl-2/immunoglobulin transcript resulting from the t(14;18) translocation. Cell. 1986; 47:19–28. [PubMed: 2875799]
6. Pezzella F, et al. bcl-2 protein in non-small-cell lung carcinoma. The New England journal of medicine. 1993; 329:690–694. [PubMed: 8393963]
7. Bredow S, Juri DE, Cardon K, Tesfaigzi Y. Identification of a novel Bcl-2 promoter region that counteracts in a p53-dependent manner the inhibitory P2 region. Gene. 2007; 404:110–116. [PubMed: 17913397]
8. Wu Y, Mehew JW, Heckman CA, Arcinas M, Boxer LM. Negative regulation of bcl-2 expression by p53 in hematopoietic cells. Oncogene. 2001; 20:240–251. [PubMed: 11313951]
9. Miyashita T, Harigai M, Hanada M, Reed JC. Identification of a p53-dependent negative response element in the bcl-2 gene. Cancer research. 1994; 54:3131–3135. [PubMed: 8205530]
10. Vousden KH, Lane DP. p53 in health and disease. Nature reviews. Molecular cell biology. 2007; 8:275–283. [PubMed: 17380161]
11. Young RL, Korsmeyer SJ. A negative regulatory element in the bcl-2 5'-untranslated region inhibits expression from an upstream promoter. Molecular and cellular biology. 1993; 13:3686–3697. [PubMed: 8388542]

12. Tsujimoto Y, Croce CM. Analysis of the structure, transcripts, and protein products of bcl-2, the gene involved in human follicular lymphoma. Proc Natl Acad Sci U S A. 1986; 83:5214–5218. [PubMed: 3523487]
13. Bredow S, Juri DE, Cardon K, Tesfaigzi Y. Identification of a novel Bcl-2 promoter region that counteracts in a p53-dependent manner the inhibitory P2 region. Gene. 2007; 404:110–116. [PubMed: 17913397]
14. Tesfaigzi Y, Fischer MJ, Martin AJ, Seagrave J. Bcl-2 in LPS- and allergen-induced hyperplastic mucous cells in airway epithelia of Brown Norway rats. Am J Physiol Lung Cell Mol Physiol. 2000; 279:L1210–L1217. [PubMed: 11076811]
15. Tesfaigzi Y, Harris JF, Hotchkiss JA, Harkema JR. DNA synthesis and Bcl-2 expression during the development of mucous cell metaplasia in airway epithelium of rats exposed to LPS. Am J Physiol Lung Cell Mol Physiol. 2004; 286:L268–L274. [PubMed: 14527929]
16. Harris JF, et al. Bcl-2 sustains increased mucous and epithelial cell numbers in metaplastic airway epithelium. American journal of respiratory and critical care medicine. 2005; 171:764–772. [PubMed: 15618464]
17. Chand HS, Woldegiorgis Z, Schwalm K, McDonald J, Tesfaigzi Y. Acute Inflammation Induces Insulin-like Growth Factor-1 to Mediate Bcl-2 and Muc5ac Expression in Airway Epithelial Cells. American journal of respiratory cell and molecular biology. 2012; 47:784–791. [PubMed: 22878411]
18. Vignola AM, et al. Proliferation and activation of bronchial epithelial cells in corticosteroid-dependent asthma. The Journal of allergy and clinical immunology. 2001; 108:738–746. [PubMed: 11692098]
19. National Heart Lung and Blood Institute & Health, N.I.o. NHLBI/WHO workshop report. Bethesda, MD: NIH; 2001. Global Initiative for Chronic Obstructive Lung Disease (GOLD) guidelines, global strategy for the diagnosis, management and prevention of chronic obstructive lung disease; p. 2701
20. Kim V, Criner GJ. Chronic Bronchitis and COPD. American journal of respiratory and critical care medicine. 2012
21. Spira A, et al. Effects of cigarette smoke on the human airway epithelial cell transcriptome. Proc Natl Acad Sci U S A. 2004; 101:10143–10148. [PubMed: 15210990]
22. Seemungal TA, Donaldson GC, Bhowmik A, Jeffries DJ, Wedzicha JA. Time course and recovery of exacerbations in patients with chronic obstructive pulmonary disease. American journal of respiratory and critical care medicine. 2000; 161:1608–1613. [PubMed: 10806163]
23. Prescott E, Lange P, Vestbo J. Chronic mucus hypersecretion in COPD and death from pulmonary infection. The European respiratory journal. 1995; 8:1333–1338. [PubMed: 7489800]
24. Spencer S, Jones PW. Time course of recovery of health status following an infective exacerbation of chronic bronchitis. Thorax. 2003; 58:589–593. [PubMed: 12832673]
25. Montes de Oca M, et al. Chronic bronchitis phenotype in subjects with and without COPD: the PLATINO study. The European respiratory journal. 2012
26. Lange P, Nyboe J, Appleyard M, Jensen G, Schnohr P. Ventilatory function and chronic mucus hypersecretion as predictors of death from lung cancer. Am Rev Respir Dis. 1990; 141:613–617. [PubMed: 2310094]
27. Brenner DR, et al. Previous lung diseases and lung cancer risk: a pooled analysis from the International Lung Cancer Consortium. American journal of epidemiology. 2012; 176:573–585. [PubMed: 22986146]
28. Hogg JC, et al. Survival after lung volume reduction in chronic obstructive pulmonary disease: insights from small airway pathology. American journal of respiratory and critical care medicine. 2007; 176:454–459. [PubMed: 17556723]
29. Chand HS, et al. Intracellular Insulin-like Growth Factor-1 Induces Bcl-2 Expression in Airway Epithelial Cells. J Immunol. 2012
30. Boers JE, ten Velde GP, Thunnissen FB. P53 in squamous metaplasia: a marker for risk of respiratory tract carcinoma. American journal of respiratory and critical care medicine. 1996; 153:411–416. [PubMed: 8542151]

31. Smith MD, Ensor EA, Coffin RS, Boxer LM, Latchman DS. Bcl-2 transcription from the proximal P2 promoter is activated in neuronal cells by the Brn-3a POU family transcription factor. The Journal of biological chemistry. 1998; 273:16715–16722. [PubMed: 9642226]
32. Venot C, et al. The requirement for the p53 proline-rich functional domain for mediation of apoptosis is correlated with specific PIG3 gene transactivation and with transcriptional repression. The EMBO journal. 1998; 17:4668–4679. [PubMed: 9707426]
33. Thomas M, et al. Two polymorphic variants of wild-type p53 differ biochemically and biologically. Molecular and cellular biology. 1999; 19:1092–1100. [PubMed: 9891044]
34. Hancox RJ, et al. Accelerated decline in lung function in cigarette smokers is associated with TP53/MDM2 polymorphisms. Hum Genet. 2009; 126:559–565. [PubMed: 19521721]
35. Imboden M, et al. Decreased PM10 exposure attenuates age-related lung function decline: genetic variants in p53, p21, and CCND1 modify this effect. Environmental health perspectives. 2009; 117:1420–1427. [PubMed: 19750108]
36. Committee. A statement by the Committee on Diagnostic Standards for Nontuberculous Respiratory Diseases. Am Rev Respir Dis. 1962; 85:762.
37. Park KS, et al. SPDEF regulates goblet cell hyperplasia in the airway epithelium. The Journal of clinical investigation. 2007; 117:978–988. [PubMed: 17347682]
38. Chen G, et al. SPDEF is required for mouse pulmonary goblet cell differentiation and regulates a network of genes associated with mucus production. The Journal of clinical investigation. 2009; 119:2914–2924. [PubMed: 19759516]
39. Wang B, Xiao Z, Ren EC. Redefining the p53 response element. Proc Natl Acad Sci U S A. 2009; 106:14373–14378. [PubMed: 19597154]
40. Youle RJ, Strasser A. The BCL-2 protein family: opposing activities that mediate cell death. Nature reviews. Molecular cell biology. 2008; 9:47–59. [PubMed: 18097445]
41. Toledo F, et al. A mouse p53 mutant lacking the proline-rich domain rescues Mdm4 deficiency and provides insight into the Mdm2-Mdm4-p53 regulatory network. Cancer cell. 2006; 9:273–285. [PubMed: 16616333]
42. Toledo F, et al. Mouse mutants reveal that putative protein interaction sites in the p53 proline-rich domain are dispensable for tumor suppression. Molecular and cellular biology. 2007; 27:1425–1432. [PubMed: 17158931]
43. Contreras AU, et al. Deacetylation of p53 induces autophagy by suppressing Bmf expression. The Journal of cell biology. 2013; 201:427–437. [PubMed: 23629966]
44. Wei CL, et al. A global map of p53 transcription-factor binding sites in the human genome. Cell. 2006; 124:207–219. [PubMed: 16413492]
45. Michalak E, Villunger A, Erlacher M, Strasser A. Death squads enlisted by the tumour suppressor p53. Biochemical and biophysical research communications. 2005; 331:786–798. [PubMed: 15865934]
46. Seto M, et al. Alternative promoters and exons, somatic mutation and deregulation of the Bcl-2-Ig fusion gene in lymphoma. The EMBO journal. 1988; 7:123–131. [PubMed: 2834197]
47. Schiavone N, et al. A conserved AU-rich element in the 3' untranslated region of bcl-2 mRNA is endowed with a destabilizing function that is involved in bcl-2 down-regulation during apoptosis. Faseb J. 2000; 14:174–184. [PubMed: 10627292]
48. Donnini M, et al. Identification of TINO: a new evolutionarily conserved BCL-2 AU-rich element RNA-binding protein. The Journal of biological chemistry. 2004; 279:20154–20166. [PubMed: 14769789]
49. Sengupta TK, Bandyopadhyay S, Fernandes DJ, Spicer EK. Identification of nucleolin as an AU-rich element binding protein involved in bcl-2 mRNA stabilization. The Journal of biological chemistry. 2004; 279:10855–10863. [PubMed: 14679209]
50. Miller SJ, Suthiphongchai T, Zambetti GP, Ewen ME. p53 binds selectively to the 5' untranslated region of cdk4, an RNA element necessary and sufficient for transforming growth factor beta- and p53-mediated translational inhibition of cdk4. Molecular and cellular biology. 2000; 20:8420–8431. [PubMed: 11046139]

51. Olsson A, Manzl C, Strasser A, Villunger A. How important are post-translational modifications in p53 for selectivity in target-gene transcription and tumour suppression? Cell death and differentiation. 2007; 14:1561–1575. [PubMed: 17627286]
52. Frank AK, et al. The codon 72 polymorphism of p53 regulates interaction with NF-{kappa}B and transactivation of genes involved in immunity and inflammation. Molecular and cellular biology. 2011; 31:1201–1213. [PubMed: 21245379]
53. Walker KK, Levine AJ. Identification of a novel p53 functional domain that is necessary for efficient growth suppression. Proc Natl Acad Sci U S A. 1996; 93:15335–15340. [PubMed: 8986812]
54. Schneider-Stock R, et al. Retention of the arginine allele in codon 72 of the p53 gene correlates with poor apoptosis in head and neck cancer. Am J Pathol. 2004; 164:1233–1241. [PubMed: 15039212]
55. Gray T, et al. Regulation of MUC5AC mucin secretion and airway surface liquid metabolism by IL-1beta in human bronchial epithelia. Am J Physiol Lung Cell Mol Physiol. 2004; 286:L320–L330. [PubMed: 14527933]
56. Fischer BM, Voynow JA. Neutrophil elastase induces MUC5AC gene expression in airway epithelium via a pathway involving reactive oxygen species. American journal of respiratory cell and molecular biology. 2002; 26:447–452. [PubMed: 11919081]
57. Harris JF, et al. Bcl-2 sustains increased mucous and epithelial cell numbers in metaplastic airway epithelium. American journal of respiratory and critical care medicine. 2005; 171:764–772. [PubMed: 15618464]
58. Dumont P, Leu JI, Della Pietra AC 3rd, George DL, Murphy M. The codon 72 polymorphic variants of p53 have markedly different apoptotic potential. Nat Genet. 2003; 33:357–365. [PubMed: 12567188]
59. Pietsch EC, Humbey O, Murphy ME. Polymorphisms in the p53 pathway. Oncogene. 2006; 25:1602–1611. [PubMed: 16550160]
60. Tuveson D, Hanahan D. Translational medicine: Cancer lessons from mice to humans. Nature. 2011; 471:316–317. [PubMed: 21412332]
61. Chen Z, et al. A murine lung cancer co-clinical trial identifies genetic modifiers of therapeutic response. Nature. 2012
62. Hunninghake GM, et al. MMP12, lung function, and COPD in high-risk populations. The New England journal of medicine. 2009; 361:2599–2608. [PubMed: 20018959]
63. Sood A, et al. Wood Smoke–Associated Chronic Obstructive Pulmonary Disease (COPD) – Underappreciated in the United States? Am J Resp and Crit Care Med. 2009; 179:A4742.
64. Akinbami LJ, Liu X. Chronic obstructive pulmonary disease among adults aged 18 and over in the United States, 1998–2009. NCHS Data Brief. 2011; 1:8.
65. Silverman EK, et al. Gender-related differences in severe, early-onset chronic obstructive pulmonary disease. American journal of respiratory and critical care medicine. 2000; 162:2152–2158. [PubMed: 11112130]
66. You Y, Richer EJ, Huang T, Brody SL. Growth and differentiation of mouse tracheal epithelial cells: selection of a proliferative population. Am J Physiol Lung Cell Mol Physiol. 2002; 283:L1315–L1321. [PubMed: 12388377]
67. Lundberg AS, et al. Immortalization and transformation of primary human airway epithelial cells by gene transfer. Oncogene. 2002; 21:4577–4586. [PubMed: 12085236]
68. Stout B, et al. STAT1 activation causes translocation of Bax to the endoplasmic reticulum during the resolution of airway mucous cell hyperplasia by IFNγ. J Immunol. 2007; 178:8107–8116. [PubMed: 17548649]
69. Tesfaigzi J, Smith-Harrison W, Carlson DM. A simple method for reusing Western blots on PVDF membranes. BioTechniques. 1994; 17:268–269. [PubMed: 7980922]
70. Niranjanakumari S, Lasda E, Brazas R, Garcia-Blanco MA. Reversible cross-linking combined with immunoprecipitation to study RNA-protein interactions in vivo. Methods. 2002; 26:182–190. [PubMed: 12054895]

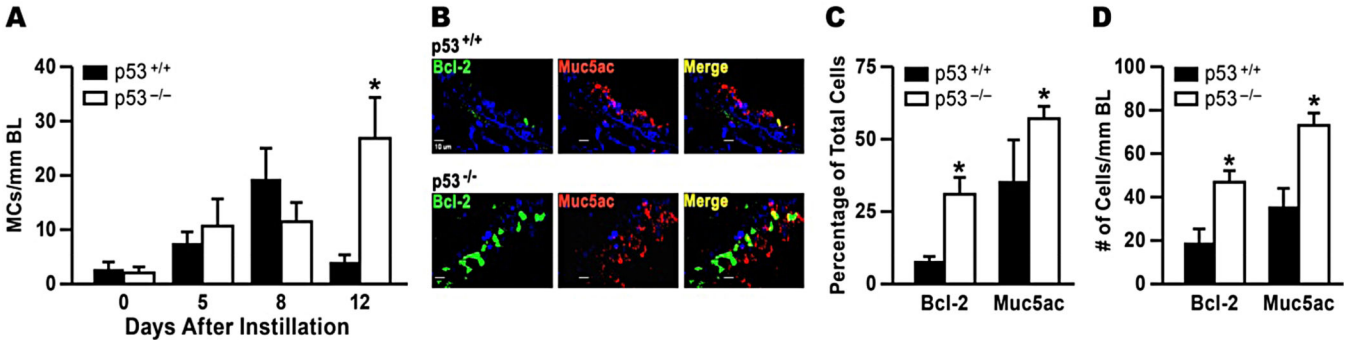

Figure 1. MCM is sustained longer in *p53*$^{-/-}$ compared to *p53*$^{+/+}$ mice

(A) *p53*$^{+/+}$ and *p53*$^{-/-}$ were instilled with LPS and MCM was quantified after 5, 8, and 12d of instillation. MC/mm basal lamina is reduced in *p53*$^{+/+}$ but is sustained in *p53*$^{-/-}$ mice at 12 d following LPS instillation. **(B)** Lung tissue sections from *p53*$^{+/+}$ and *p53*$^{-/-}$ mice at 12d post instillation were immunostained with antibodies to Bcl-2 and Muc5ac and with DAPI to visualize nuclei (scale bar 10 μm). **(C)** Percentages for Bcl-2- and Muc5ac-positive cells. **(D)** Cell numbers of Bcl-2- and Muc5ac-positive cells per millimeter basal lamina. Bars = group means ± standard error from the mean (n = 3–5 mice/group); * P<0.05.

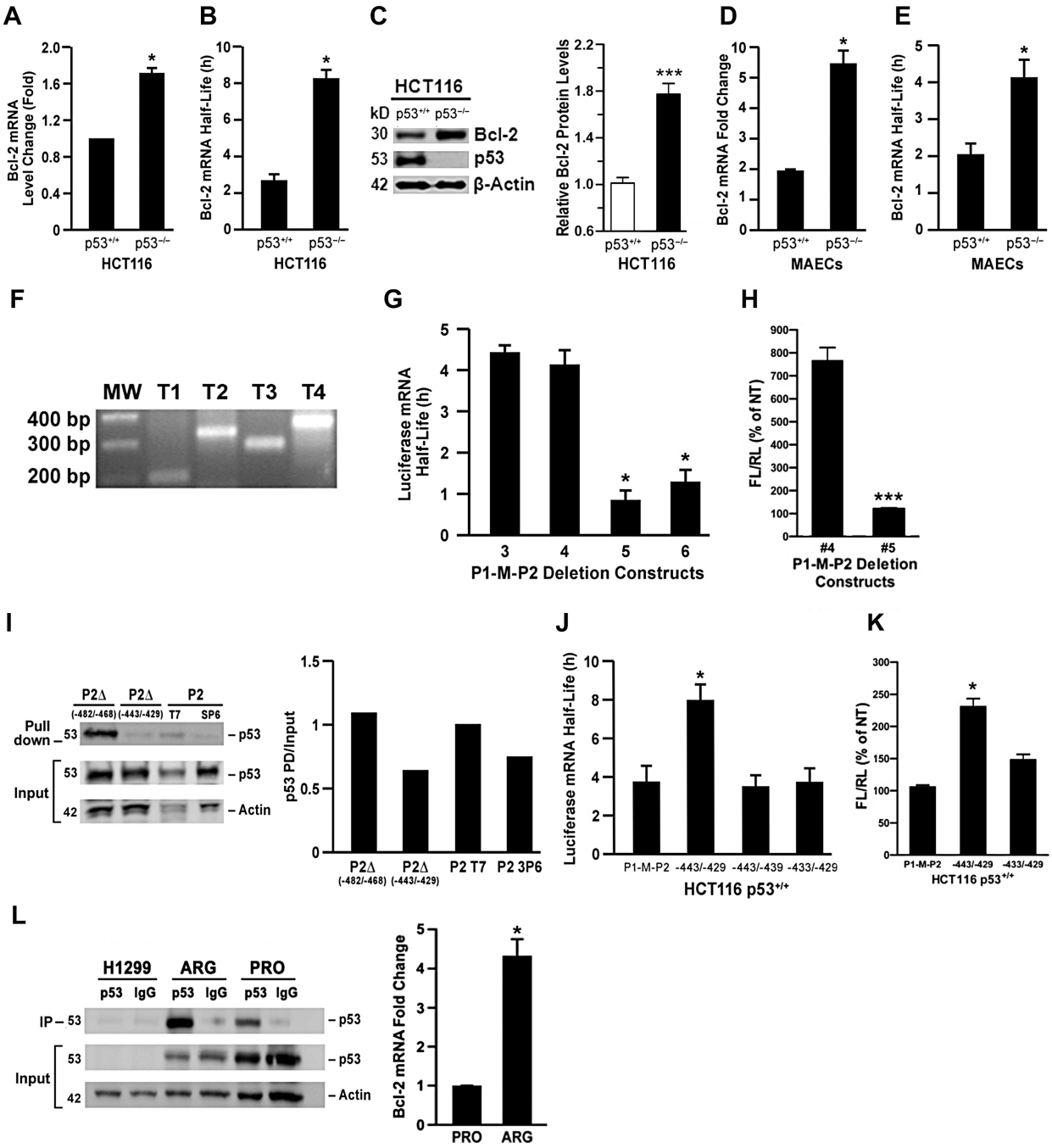

Figure 2. p53 reduces Bcl-2 protein and mRNA levels by destabilizing *bcl-2* mRNA

(A) *Bcl-2* mRNA levels in $p53^{+/+}$ and $p53^{-/-}$ HCT116 quantified by qRT-PCR. **(B)** *Bcl-2* mRNA half-life in $p53^{+/+}$ and $p53^{-/-}$ HCT116 cells determined after DRB treatment for 0, 2, 4, 6, and 8h and Bcl-2 mRNA quantified by qRT-PCR. **(C)** Bcl-2 protein levels in $p53^{+/+}$ and $p53^{-/-}$ HCT116 cells with densitometric quantification normalized to actin content shown in the lower panel. **(D)** *Bcl-2* mRNA levels and mRNA half-life **(E)** in $p53^{-/-}$ and $p53^{+/+}$ primary mouse airway epithelial cells (MAECs). **(F)** RT-PCR for T1, T2, T3 and T4 *bcl-2* transcripts of HAECs. **(G)** Luciferase mRNA half-life analyzed in H1299p53^{ts} cells

transfected with P1MP2-Δ3, Δ4, Δ5, and Δ6 -luciferase constructs, treated with DRB at 16 h post-transfection and RNA collected at 0, 2, 4, and 6h. **(H)** Luciferase activity for P1MP2-Δ4 and Δ5 constructs measured using firefly (FL) to renilla (RL) luciferase ratio. **(I)** The P2 region cloned in the pCRII dual promoter vector was used to generate Bio-11-UTP-labeled sense and anti-sense RNA using the T7 and Sp6 promoters, respectively; the labeled RNAs were pull-down using H1299p53^{ts} S-100 cytosolic extracts. p53 was detected in pull-down products using sense (lane 3) but not anti-sense RNA (lane 4). Bio-11-UTP-labeled sense RNA prepared from two deletions introduced into the P2-containing constructs - pCR-II P2(−482/−468) and pCR-II P2(−443/−429). Pull-down assays performed with sense RNA from pCR-II P2(−482/−468) (lane 1), pCR-II P2(−443/−429) (lane 2). Densitometric quantification of pull-down products normalized to the input shown in left panel. **(J)** Luciferase mRNA half-life for P1MP2Δ(−443/−429,−443/−439,−433/−429) luciferase and wild-type P1MP2 luciferase vectors following transfection into HCT116 p53$^{+/+}$ cells **(K)** The luciferase activity for wild-type P1MP2 luciferase and P1MP2Δ−443/−439,−433/−429) luciferase constructs. **(L)** Cell extracts prepared from H1299 and H1299p53ts cells maintained at 32°C were immunoprecipitated using anti-p53 or IgG_1 and probed for p53 on a Western blot. Analysis of pull-down products for *bcl-2* mRNA by qRT-PCR was normalized to the total protein and input. Bars = group means ± standard error from the mean (n = 3 different treatments/group); * P<0.05.

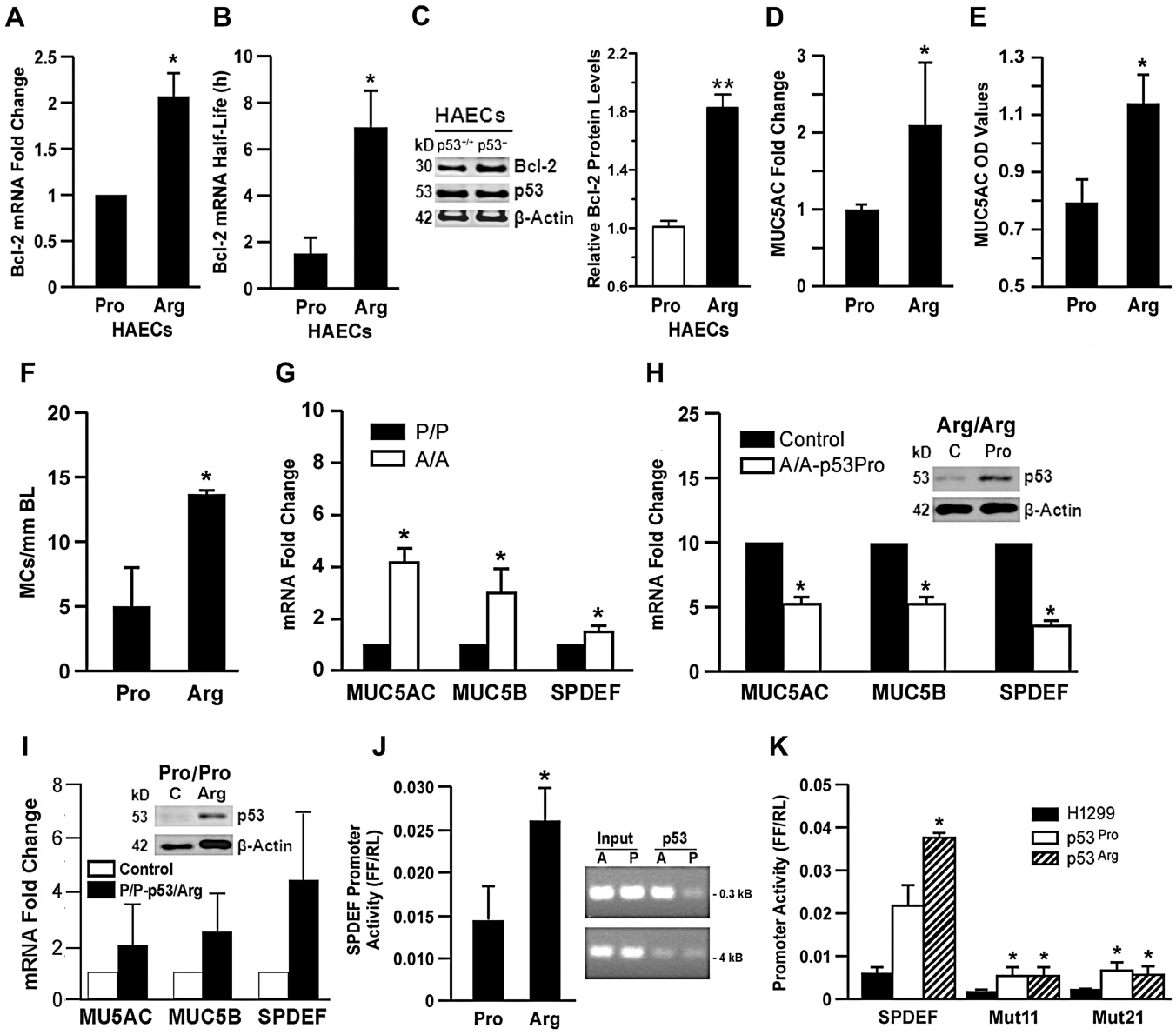

Figure 3. p53^{Arg} interacts and upregulates SPDEF to stimulate the mucous regulatory network

(A) Bcl-2 mRNA levels in primary HAEC^{Arg} and HAEC^{Pro} cultures. **(B)** Bcl-2 mRNA half-life in primary HAECs 2 h after activating p53 by exposing cells to 10 mJ UV. HAECs from three individuals with p53^{Arg} or the p53^{Pro} variants were treated with DRB and Bcl-2 mRNA half-life was determined at 0, 2, 4, 6, and 8h. **(C)** Bcl-2 protein levels in HAEC^{Arg} and HAEC^{Pro} cells with densitometric quantification normalized to actin content shown in the lower panel. **(D)** Comparison of MUC5AC mRNA levels by qRT-PCR in HAEC^{Arg} and HAEC^{Pro} cultures from 10 individuals each. HAECs were differentiated on ALI cultures. **(E)** MUC5AC protein in washes from HAEC^{Arg} and HAEC^{Pro} cultures from 10 individuals each determined by ELISA. **(F)** The number of mucous cells per mm basal lamina determined by counting cells using morphometry. **(G)** Validation of expression of MUC5AC, MUC5B, and SPDEF mRNAs by qRT-PCR based on microarray results from HAEC^{Arg} and HAEC^{Pro} cultures from 10 individuals each. **(H)** Expression of p53^{Pro} in

HAEC^{Arg} cells using adenoviral expression vector reduces expression of MUC5AC, MUC5B, and SPDEF. **(I)** Expression of p53^{Arg} in HAEC^{Pro} cells using adenoviral expression vector increases expression of MUC5AC, MUC5B, and SPDEF. **(J)** SPDEF promoter in pGL3Basic exhibits a higher promoter activity in the H1299^{ts}Arg cells compared to H1299^{ts}Pro cells. **(K)** ChIP assay using p53 antibodies from H1299^{ts}Arg and H1299^{ts}Pro cells showed that significantly more DNA was pulled down from the Arg cells compared to the Pro cells. Input denotes that similar DNA amounts were used for the pull-down experiment. Interaction of p53 is visible when using primers specific to the −0.3 kB region but absent when using primers specific to the −4kB region. **(L)** H1299, H1299^{ts}Arg and H1299^{ts}Pro cells transfected with promoter constructs for SPDEF, deletion mutant 11 and deletion mutant 12 in pGL3Basic and promoter activities were measured. Promoter activity was reduced for both cell types with both mutants. Bars = group means ± standard error from the mean (n = 3 different treatments/group). *P<0.05.

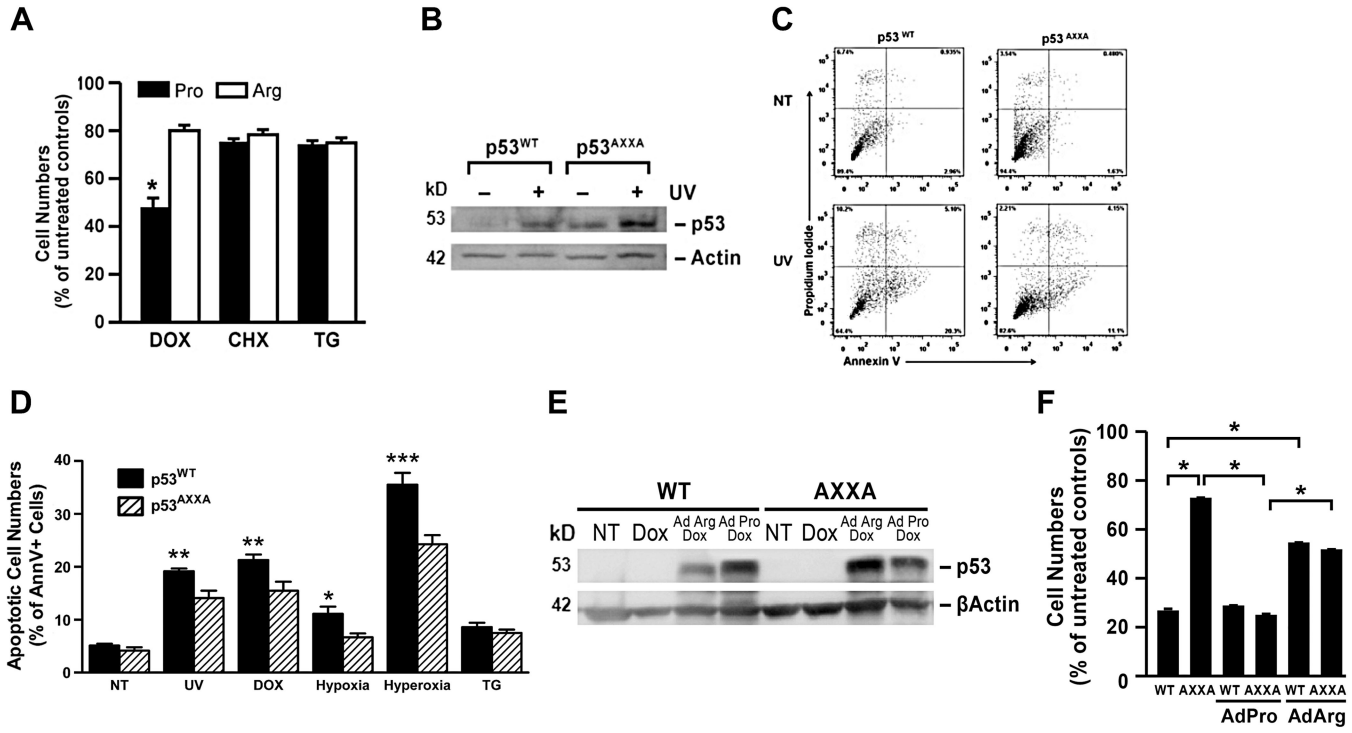

Figure 4. The proline-rich domain of p53 affects DNA damage-induced cell death in airway epithelial cells

(A) H1299p53^{ts}Arg and H1299p53^{ts}Pro cells treated with 50 ng/ml DRB, and either 1 μM doxorubicin, 10 μM cyclohexamide, or 1 μM thapsigargin, and cell numbers quantified 48 h later. **(B)** p53 levels were increased in p53^{WT} and p53^{AXXA} MEFs when treated with 10 mJ UV irradiation. **(C)** p53^{WT} and p53^{AXXA} MEFs treated with 10 mJ UV irradiation in the presence of 50 ng/ml DRB and cell death analyzed by Annexin V and propidium iodide (PI) staining. **(D)** Quantification of Annexin V-positive cells in p53^{WT} and p53^{AXXA} MEFs following treatment for 8 h with 50 ng/ml DRB and either 10 mJ UV irradiation, 1 μM doxorubicin, 5% O_2 (hypoxia), 95% O_2 (hyperoxia), or 1 μM thapsigargin. **(E)** Western blot verifying the presence of p53 after infection of p53^{WT} and p53^{AXXA} MEFs with adenoviral vectors expressing p53^{Arg} or p53^{Pro}. **(F)** p53^{WT} and p53^{AXXA} MEFs were either left untreated (control) or infected with adenoviral vectors for p53^{Arg} or p53^{Pro} then treated with 1μM doxorubicin for 24 h and cell numbers quantified. Bars = group means ± standard error from the mean (n = 3 different treatments/group) ; * P<0.05; ** P<0.01.

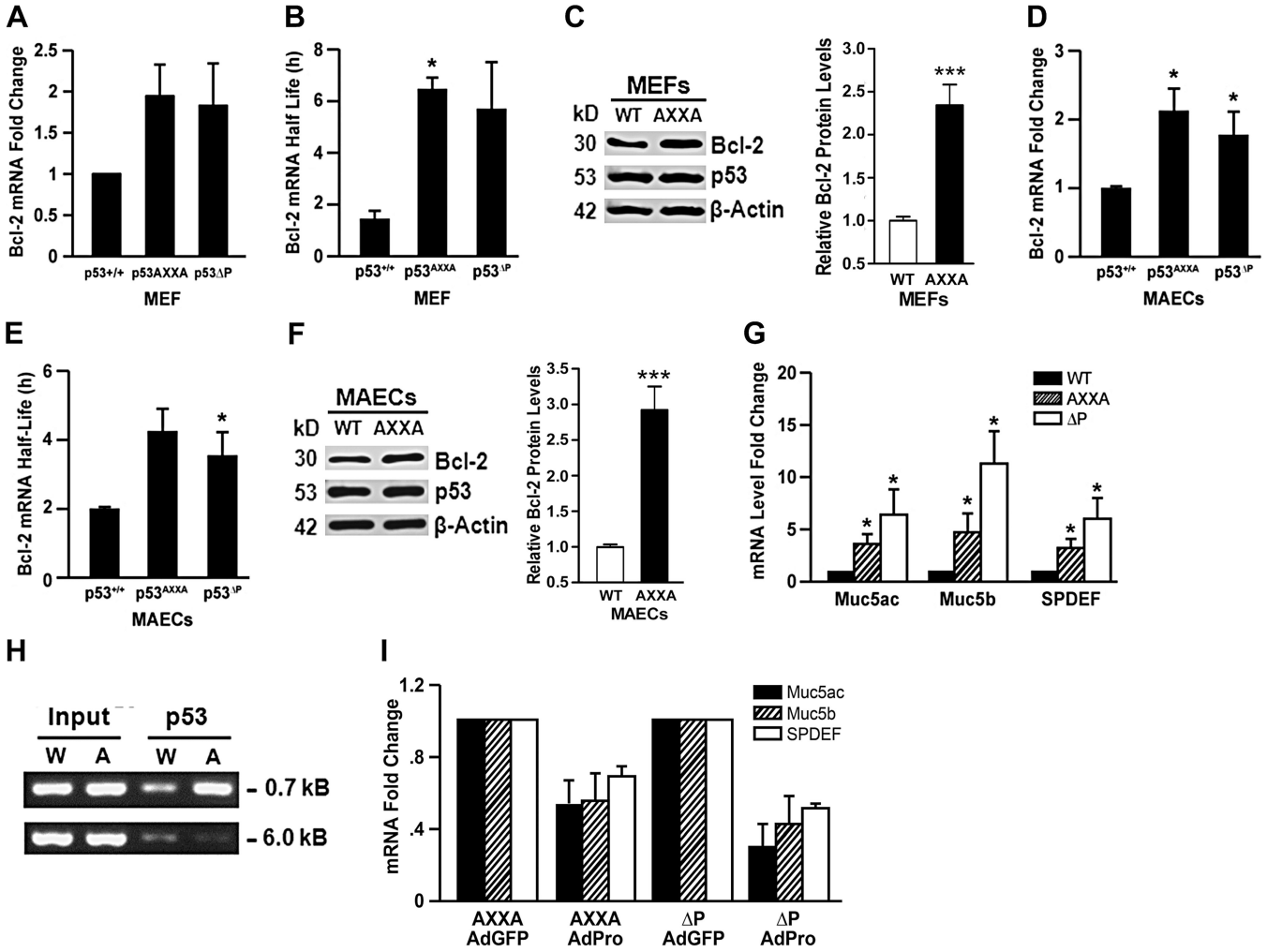

Figure 5. The proline-rich domain of murine p53 regulates *bcl-2* mRNA levels and half-life, and the expression of mucous differentiation genes

Bcl-2 mRNA levels **(A, D)** and mRNA half-life **(B, E)** in MEFs **(A, B)** and in MAECs **(D, E)**, respectively from $p53^{WT}$, $p53^{\Delta P}$, and $p53^{AXXA}$ mice after treatment with 10 mJ UV light was determined after treating with DRB and collecting RNA samples at 0, 2, 4, 6, 8, 10 and 12h for analysis by qRT-PCR. Experiments were repeated at least 3 times with each experiment containing 3–4 independent repeats. Bcl-2 protein levels in MEFs **(C)** and MAECs **(F)** from $p53^{WT}$ and $p53^{AXXA}$ mice with densitometric quantification of Bcl-2 protein levels normalized to actin content shown in the lower panels. **(G)** MAECs isolated from $p53^{WT}$, $p53^{AXXA}$ and $p53^{\Delta P/\Delta P}$ mice were differentiated on air-liquid interface cultures on Transwell membranes and RNA analyzed by qRT-PCR for *Muc5ac*, *Muc5b*, and *SPDEF*. **(H)** ChIP assay using p53 antibodies from $p53^{WT}$ and $p53^{AXXA}$ MEFs showed that significantly more DNA was pulled down from the AXXA cells compared to the WT cells. Input denotes that similar DNA amounts were used for the pull-down experiment. Interaction of p53 is visible when using primers specific to the −0.7 kB region but absent when using primers specific to the −6 kB region. **(I)** $p53^{AXXA}$ and $p53^{\Delta P}$ MAECs were differentiated on air-liquid interface cultures and infected with adenoviruses AdGFP

(control) and AdPro. Isolated RNA was analyzed by qRT-PCR for *Muc5ac*, *Muc5b*, and *SPDEF*. Bars = group means ± standard error from the mean (n = 3 different treatments/group); * $P<0.05$.

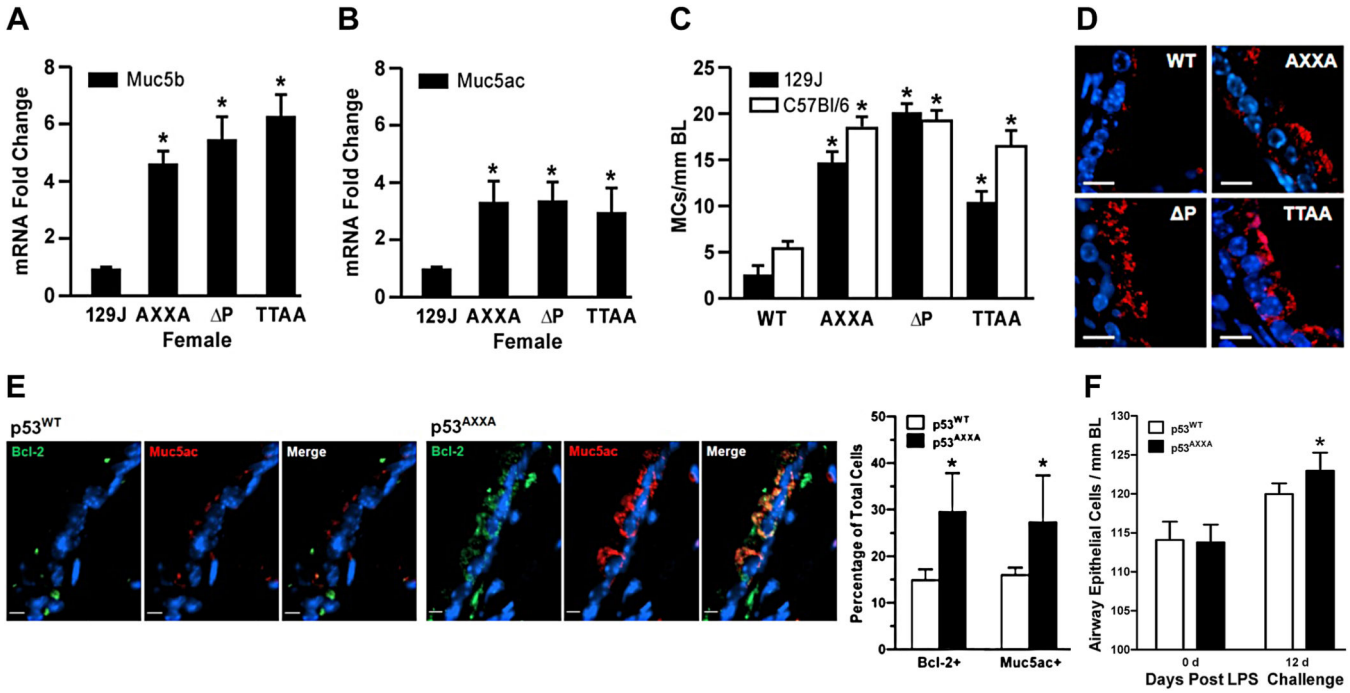

Figure 6. The proline-rich domain of p53 is crucial in regulating mucous differentiation

RNA from the right cranial lung lobes of $p53^{WT}$, $p53^{AXXA}$ and $p53^{\Delta P}$ mice were analyzed by qRT-PCR for Muc5b **(A)** and Muc5ac **(B)**. **(C)** Mucous cells per mm basal lamina were quantified in the axial airways of $p53^{WT}$, $p53^{AXXA}$, $p53^{\Delta P}$, and $p53^{TTAA}$ mice on 129J and C57Bl/6 backgrounds. Bars = group means ± standard error from the mean (n = 6 mice/group). * denotes statistically significant difference. **(D)** Representative micrographs of airway tissue sections from $p53^{WT}$, $p53^{AXXA}$, $p53^{\Delta P}$, and $p53^{TTAA}$ mice on 129J immunostained for Muc5ac (red) and counterstained with DAPI (blue) for nuclear staining. Scale - 10 μm. **(E)** *$p53^{WT}$* and *$p53^{AXXA}$* mice were instilled with LPS and changes in Bcl-2- and Muc5ac-positive cells was quantified after 12d of instillation. Representative micrographs from $p53^{WT}$ and $p53^{AXXA}$ mice airway sections at 12 d post LPS instillation showing the Bcl-2 (green) and Muc5ac (red) immunostained cells and with DAPI (blue) nuclear counterstaining. Scale - 5 μm. **(F)** Total airway epithelial cell numbers per millimeter basal lamina at 0 d (baseline) and at 12 d post LPS instillation. Bars = group means ± standard error from the mean (n = > 3 mice/group); * $P<0.05$.